Atmospheric peroxyacetyl nitrate (PAN): a global budget and source attribution

E.V. Fischer[1], D. J. Jacob[2], R. M. Yantosca[2], M. P. Sulprizio[2], D. B. Millet[3], J. Mao[4], F. Paulot[1], H. B. Singh[5], A. Roiger[6], L. Ries[8], R.W. Talbot[7], K. Dzepina[9], and S. Pandey Deolal[10]

[1] Department of Atmospheric Science, Colorado State University, Fort Collins, CO, USA
[2] School of Engineering and Applied Sciences, Harvard University, Cambridge, MA, USA
[3] Department of Soil, Water and Climate, University of Minnesota, St. Paul, MN, USA
[4] Princeton University, GFDL, Princeton, NJ, USA
[5] NASA Ames Research Center, Moffett Field, CA, USA
[6] German Aerospace Center, Institute of Atmospheric Physics, Atmospheric Trace Gases, Oberphaffenhofen, Germany
[7] Federal Environment Agency, GAW Global Station Zugspitze/Hohenpeissenberg, Zugspitze, Germany
[8] Department of Earth and Atmospheric Sciences, University of Houston, Houston, TX, USA
[9] Department of Chemistry, Michigan Technological University, Houghton, MI USA
[10] Bluesign Technologies AG, St. Gallen, Switzerland

January 17, 2014

Corresponding Author: Emily Fischer, evf@atmos.colostate.edu

Emily Fischer 1/8/14 10:36 PM
Deleted: .-E

Emily Fischer 1/8/14 10:36 PM
Deleted: August

Emily Fischer 1/8/14 10:36 PM
Deleted: 25

Emily Fischer 1/17/14 2:49 PM
Deleted: 2013

Abstract

Peroxyacetyl nitrate (PAN) formed in the atmospheric oxidation of non-methane volatile organic compounds (NMVOCs), is the principal tropospheric reservoir for nitrogen oxide radicals ($NO_x = NO + NO_2$). PAN enables the transport and release of NO_x to the remote troposphere with major implications for the global distributions of ozone and OH, the main tropospheric oxidants. Simulation of PAN is a challenge for global models because of the dependence of PAN on vertical transport as well as complex and uncertain NMVOC sources and chemistry. Here we use an improved representation of NMVOCs in a global 3-D chemical transport model (GEOS-Chem) and show that it can simulate PAN observations from aircraft campaigns worldwide. The immediate carbonyl precursors for PAN formation include acetaldehyde (44% of the global source), methylglyoxal (30%), acetone (7%), and a suite of other isoprene and terpene oxidation products (19%). A diversity of NMVOC emissions is responsible for PAN formation globally including isoprene (37%) and alkanes (14%). Anthropogenic sources are dominant in the extratropical northern hemisphere outside the growing season. Open fires appear to play little role except at high northern latitudes in spring, although results are very sensitive to plume chemistry and plume rise. Lightning NO_x is the dominant contributor to the observed PAN maximum in the free troposphere over the South Atlantic.

1. Introduction

Peroxyacetic nitric anhydride ($CH_3COO_2NO_2$), commonly known by its misnomer peroxyacetyl nitrate (PAN), is the principal tropospheric reservoir species for nitrogen oxide radicals ($NO_x = NO + NO_2$) with important implications for the production of tropospheric ozone (O_3) and of the hydroxyl radical OH (the main atmospheric oxidant) (Singh and Hanst, 1981). PAN is formed by oxidation of non-methane volatile organic compounds (NMVOCs) in the presence of NO_x. NMVOCs and NO_x have both natural and anthropogenic sources. Fossil fuel combustion is the principal NO_x source with additional contributions from biomass burning, lightning and soils (van der A et al., 2008). The organic side of PAN formation involves many stages of NMVOC oxidation. Most NMVOCs can serve as PAN precursors but the yields vary widely (Roberts, 2007).

PAN enables the long-range transport of NO_x at cold temperatures, and PAN decomposition releases NO_x in the remote troposphere where it is most efficient at producing O_3 and OH (Singh and Hanst, 1981; Hudman et al., 2004; Fischer et al., 2010; Singh, 1987). NO_x abundance controls the balance of O_3 production and destruction. Without PAN formation the distributions of tropospheric NO_x, O_3 and OH would be very different, with higher values in NO_x source regions and lower values in the remote troposphere (Kasibhatla et al., 1993; Moxim et al., 1996; Wang et al., 1998a). PAN chemistry can also be important for oxidant formation on a regional scale. In polluted environments, PAN formation is a sink for both NO_x and hydrogen oxide radicals (HO_x). Observations show that O_3 concentrations increase when temperature increases, and this has been in part related to PAN thermal instability (Sillman and Samson, 1995). Observations also show that the production of PAN becomes more efficient relative to O_3 in highly

Emily Fischer 1/17/14 3:15 PM
Deleted: P

Emily Fischer 1/17/14 3:15 PM
Deleted: (PAN

Emily Fischer 1/17/14 3:15 PM
Deleted: $CH_3COO_2NO_2$)

polluted air masses (Roberts et al., 1995). Thus a comprehensive understanding of PAN is needed to understand oxidant distributions on a spectrum of scales.

A large body of PAN observations worldwide has accumulated over the years, including in particular from aircraft platforms and mountaintop sites. There have also been recent retrievals of PAN concentrations in the upper troposphere from satellites (Glatthor et al., 2007; Tereszchuk et al., 2013). Concentrations vary from pptv levels in warm remote locations such as tropical oceans to ppbv levels in polluted source regions. Despite the relatively large database of measurements compared to other photochemical indicators, simulation of PAN in global chemical transport models (CTMs) has been a difficult challenge because of the complexity of PAN chemistry. Recent model inter-comparisons show very large difference among themselves and with observations in many regions of the atmosphere (Thakur et al., 1999; Singh et al., 2007, von Kuhlmann et al., 2003; Sudo et al., 2002), but confirm the very important role for PAN in sustaining O_3 production in remote air (Zhang et al., 2008; Hudman et al., 2004).

Here we exploit a worldwide collection of PAN observations to improve the PAN simulation in the GEOS-Chem CTM, which has been used extensively in global studies of tropospheric oxidants (Bey et al., 2001; Sauvage et al., 2007; Murray et al., 2012). The earliest global models that included PAN chemistry (Kasibhatla et al., 1993; Moxim et al., 1996) relied on highly simplified NMVOC budgets. Our improvements involve new treatments of NMVOC sources and chemistry, a well-known weakness even in current CTMs (Williams et al., 2013; Ito et al., 2007). Our new simulation, which captures the major features of the existing observations, affords a new opportunity to understand the factors driving the global PAN distribution and the essential chemistry that needs to be

described. A detailed analysis of how PAN shapes the global distributions of the atmospheric oxidants and nitrogen deposition will be the focus of a subsequent paper.

2. Model Description

We use the GEOS-Chem global 3-D CTM including detailed ozone-NO_x-VOC-aerosol chemistry (version 9.01.01, www.geos-chem.org) with significant modifications as described below.

2.1 Chemistry

GEOS-Chem uses a chemical scheme originally described by Horowitz et al. (1998) and Bey et al. (2001), with recent updates outlined in Mao et al. (2010). Following Marais et al. (2012) we have updated the rate coefficients for the reactions of HO_2 with the $>C_2$ peroxy radicals to Equation (iv) in Saunders et al. (2003). We also include nighttime reactions of organic peroxy radicals with NO_3 following Stone et al. (2013). To implement the Stone et al., (2013) nighttime chemistry, we went through each of the RO_2 + NO reactions in the GEOS-Chem chemical mechanism, copied each of these reactions, and changed the RO_2 reactants to react with NO_3 rather than NO. The Master Chemical Mechanism (MCM) considers three different reactions rates for this class, one for CH_3O_2, one for $RC(O)O_2$ and one for all other RO_2. There is no temperature dependence included and all products are assumed to be the same as the corresponding reaction of the RO_2 radical with NO (Bloss et al., 2005). We replaced the isoprene chemical mechanism with one based on Paulot et al. (2009a, 2009b), as described by Mao et al. (2013b).

Emily Fischer 1/12/14 12:40 PM
Formatted: Font:Not Italic

Emily Fischer 1/12/14 12:40 PM
Formatted: Font:Not Italic

Emily Fischer 1/12/14 12:40 PM
Formatted: Font:Not Italic

PAN is produced reversibly by reaction of the peroxyacetyl (PA) radical $CH_3C(O)OO$ with NO_2:

$$CH_3C(O)OO + NO_2 + M \rightleftarrows PAN + M \quad (1)$$

where M is a third body (typically N_2 or O_2). The dominant sources of $CH_3C(O)OO$ are the oxidation of acetaldehyde (CH_3CHO) and the photolysis of acetone ($CH_3C(O)CH_3$) and methylglyoxal (CH_3COCHO):

$$CH_3CHO + OH \xrightarrow{O_2} CH_3C(O)OO + H_2O \quad (2)$$

$$CH_3C(O)CH_3 + h\upsilon \xrightarrow{O_2} CH_3C(O)OO + CH_3 \quad (3)$$

$$CH_3COCHO + h\upsilon \xrightarrow{O_2} CH_3C(O)OO + HCO \quad (4)$$

PAN can also be produced at night via reaction of acetaldehyde with the nitrate radical. Acetaldehyde, acetone and methylglyoxal are all directly emitted ("primary" sources) and produced in the atmosphere from oxidation of primary emitted NMVOCs ("secondary" sources). These different sources will be discussed below. There are also other minor sources of the PA radical, again to be discussed below.

Emily Fischer 1/12/14 11:18 AM
Deleted: both

Higher acyl peroxy nitrates ($RC(O)OONO_2$) are similarly formed from the oxidation of NMVOCs, but their yields are much lower than that for PAN. We focus on PAN because observations show that it typically accounts for 75 - 90% of total acyl peroxy nitrates (Roberts, 2007; Roberts et al., 2002; Roberts et al., 1998; Wolfe et al., 2007) and there are an abundance of measurements of PAN. Closure on measurements of total reactive nitrogen oxides (NO_y) confirms the dominant role of PAN as an organic nitrate reservoir for NO_x (Roberts et al., 1995; Bertram et al., 2013).

The main sink of PAN is thermal decomposition (reaction 1), and the effective PAN lifetime depends on whether the released PA radical reacts with NO_2 to return PAN, or with another species (mainly NO or HO_2) leading to permanent loss. To describe this chemistry,

GEOS-Chem uses the recommendation from Sander et al., (2011), which is taken from Bridier et al. (1991). The parameters recommended by Bridier et al. (1991) are consistent with later studies of PAN decomposition by Roberts and Bertman (1992), Orlando et al. (1992), and Grosjean et al. (1994). The rate coefficient for the reaction of the PA radical with NO is also from Tyndall et al. (2001).

Emily Fischer 1/12/14 1:02 PM
Deleted: the equilibrium constant given in Tyndall et al. (2001) to describe the cycling between PAN and the PA radical

Emily Fischer 1/12/14 1:03 PM
Deleted: and Sehested et al. (1998).

Primary NMVOCs in the standard GEOS-Chem mechanism that contribute to PAN formation include ethane, propane, $>C_3$ alkanes (lumped), $>C_2$ alkenes (lumped), isoprene, acetaldehyde, methylglyoxal, acetone, and $>C_3$ ketones (lumped). Our extended mechanism adds several additional primary NMVOCS including ethanol, benzene, toluene and ethylbenzene (lumped), xylenes and trimethyl benzenes (lumped), and monoterpenes (lumped). The additions were partially motivated by the work of Ito et al. (2007) who extended the GEOS-Chem mechanism within the IMPACT CTM to include a broader suite of NMVOCs. One result of this exercise was a dramatic increase in PAN formation through methylglyoxal and hydroxyacetone. Liu et al. (2010) found aromatics to be a major source of PAN in urban China through the production of methylglyoxal. We calculate the associated yield of methylglyoxal using recommended values for the individual aromatic species (toluene, o-xylene, m-xylene, p-xylene, 1,2,3-trimethylbenzene, 1,2,4-trimethylbenzene, and 1,3,5-trimethylbenzene) from Nishino et al. (2010) and the observed mean aromatic speciation for Chinese cities from Barletta et al. (2006).

We adopted the treatment of monoterpene oxidation from the RACM2 chemical mechanism (Goliff et al., 2013), lumping terpenes with one double bond (alpha-pinene, beta-pinene, sabinene and delta-3-carene) into one proxy. Unlike Ito et al. (2007), hydroxyacetone is not a product of terpene oxidation in the revised RACM2 mechanism

used here. The gas phase oxidation of monoterpenes is highly unconstrained. The RACM2 mechanism is primarily based on Atkinson and Avery (2003). The yields of the immediate PAN precursors resulting from terpene degradation as described by RACM2 embedded in GEOS-Chem are given in Table 1. The mechanism produces methyl ethyl ketone and acetone, both of which can serve as PA radical precursors. The addition of this lumped terpene increases PAN in the model. The largest surface changes for PAN are for Eastern Europe and Western Russia, where there are high biogenic terpene emissions but there is little PAN data for comparison.

Emily Fischer 1/12/14 8:11 PM
Formatted: Font:Not Italic

In addition to thermal decomposition, we include minor sinks for PAN from dry deposition and photolysis. The dry deposition velocity for PAN is simulated using a standard resistance-in-series approach (Wesely, 1989) as implemented in GEOS-Chem by Wang et al. (1998b). We assume that the PAN reactivity with surfaces is as strong as that of O_3 (Shepson et al., 1992), but we explore the sensitivity to this choice. Photolysis and deposition account globally for 1.8% and 1.2% of the global PAN sink respectively. Photolysis of PAN is important in the upper troposphere where the lifetime against loss via photolysis is on the order of a month (Talukdar et al., 1995). We find that assuming PAN reactivity with surfaces is more similar to O_3 rather than NO_2, decreases surface PAN concentrations over northern hemisphere continents by 15-20% in spring. Reaction of PAN with both the OH radical and Cl atoms is slow, and these are both minor loss pathways, unnecessary to include in global models (Wallington et al., 1990; Talukdar et al., 1995). Uptake on ice particles in convective clouds (Marecal et al., 2010) and on organic aerosols (Roberts, 2005) are both thought to be negligible and are not included here. PAN is only sparingly soluble, but hydrolysis of the PA radical is thought to explain observed PAN loss

194 in fog (Villalta et al., 1996; Roberts et al., 1996). We do not consider this to be a significant
195 loss process for PAN on a global scale (Jacob, 2000).

196 **2.2 Emissions**

197 Production of PAN can be limited by either the supply of NO_x or NMVOCs, as
198 discussed below. Global fossil fuel emissions of NO_x in GEOS-Chem are from the EDGAR
199 inventory (Oliver and Berdowski, 2001) and are overwritten with regional inventories for
200 Europe (EMEP) (Vestreng and Klein, 2002), Mexico (BRAVO) (Kuhns et al., 2003), East
201 Asia (Zhang et al., 2009), Canada (NPRI, http://www.ec.gc.ca/inrp-npri/), and the United
202 States (EPA/NEI2005, http://www.epa.gov/ttnchie1/net/2005inventory.html). All
203 anthropogenic NO_x emissions are scaled to 2008 based on energy statistics (van Donkelaar
204 et al., 2008). Soil NO_x emissions in GEOS-Chem are based on Yienger and Levy (1995) as
205 implemented by Wang et al. (1998b) . Lightning NO_x emissions are described by Sauvage
206 et al. (2007).

207 Table 1 lists the global emissions of all NMVOCs that contribute to PAN formation.
208 We use the RETRO (REanalysis of the TROpospheric chemical composition) emission
209 inventory (van het Bolscher et al., 2008) as global default for anthropogenic NMVOC
210 emissions aside from ethane and propane. Ethane and propane emissions in RETRO were
211 far too low compared to the GEOS-Chem inventories from Xiao et al. (2008), which are
212 unbiased relative to observations. Emissions of both species appeared to be missing from
213 the major natural gas production region in Russia. We used the ethane and propane
214 emission inventories which were developed as in Xiao et al. (2008). The RETRO emission
215 inventory is for 2000, and we scaled it to 2008 following van Donkelaar et al. (2008).
216 RETRO includes anthropogenic emissions for benzene, xylene and toluene. Based on the

observed CO to benzene ratio for TRACE-P, we increased benzene emissions over China by 25%. We then scaled xylene and toluene emissions to benzene based on measurements from 43 Chinese cities from Barletta et al. (2006). Thus RETRO emissions of toluene were increased by a factor of 4 over China to create our lumped toluene, and RETRO emissions of xylene were increased by a factor of 8 over China to create our lumped xylene species. Observations show large abundances of reactive aromatics over southern and eastern China (Ran et al., 2009; Wang et al., 2002; Zhang et al., 2007a; Wang et al., 2013).

Terrestrial biogenic emissions of acetone, acetaldehyde, isoprene, ethanol, terpenes, and $>C_2$ alkenes from metabolism and decay are calculated locally using the Model of Emissions of Gases and Aerosols from Nature (MEGAN v2.0) (Guenther et al., 2006). Specific other sources and sinks for acetone and acetaldehyde are described in Fischer et al. (2012) and Millet et al. (2010) respectively. The atmospheric budget of ethanol is also as described by Millet et al. (2010).

New estimates indicate that fires emit significantly more NMVOCs than previously thought (Wiedinmyer et al., 2011), and there is a large contribution from oxygenated species, many of which are unidentified (Warneke et al., 2011). Observations show rapid conversion of NO_x to PAN in fire plumes, seemingly due to the oxidation of very short-lived NMVOCs (Jacob et al., 1992). We use 2008 Global Fire Emissions Database (GFED3) monthly biomass burning emissions for NO_x and NMVOCs (van der Werf et al., 2010) with updated emission factors for NMVOCs and NO_x from extratropical forests, savannas and agricultural fires from Akagi et al. (2011). The updated NO_x emission factor for extratropical fires is approximately a factor of three lower, and the emission factors for the NMVOCs are generally higher. Following Alvarado et al. (2010) we directly partition 40% and 20% NO_x

emissions from fires directly to PAN and HNO_3, respectively. The Alvarado et al. (2010) partitioning is based on an observation of fresh boreal fire plumes, but we apply it here to all fire types. Our additional NMVOC budgets include the addition of biomass burning emissions as given in Table 1.

The standard version of GEOS-Chem releases all fire emissions in the boundary layer; however, previous studies have pointed out that a significant fraction of biomass burning emissions can be injected to the free troposphere because of buoyancy (Turquety et al., 2007; Val Martin et al., 2010). This is especially important for PAN because lower temperatures above the boundary layer enhance its stability. Val Martin et al. (2010) showed that a substantial fraction of plumes from North American fires are injected into the free troposphere. Smoke plumes over the boreal region reached the highest altitudes. Analysis of smoke clouds, which are a later stage of plume evolution, indicated that ~35% were above the boundary layer. Here we distribute 35% of biomass burning emissions by mass in the 10 sigma layers (4 km) above the boundary layer, and this improves our comparison with PAN observations at high latitudes. The PAN simulation is sensitive to this choice.

Kaiser et al. (2012) and Yue et al. (personal communication) find that GFED3 underestimates fire emissions by not accounting for small fires, particularly at boreal latitudes. Following their work, we increased wild fire emissions by 60% in North Asia (30 – 75°N, 60 – 190°E), 25% in Canada and 50% in Alaska. Increasing fire emissions over Russian and North American boreal regions improves the PAN simulation over the Arctic, particularly above the surface

2.3. Model Configuration

Emily Fischer 1/12/14 1:17 PM
Deleted: To support PA radical formation on faster

Emily Fischer 1/12/14 1:18 PM
Deleted: timescales we also added GFED3 emissions of several shorter lived hydrocarbons to the suite of species emitted from fires (terpenes, aromatics) along with additional oxygenated species (hydroxyacetone, methylgloyxal)

In our work GEOS-Chem is driven by NASA GEOS-5 assimilated meteorological data with 0.5° x 0.67° horizontal resolution, 47 levels in the vertical, and 3–6 hour temporal resolution. We degrade the horizontal resolution to 2° x 2.5° for input into our GEOS-Chem simulation. We use a 1-year simulation for 2008, preceded by a 1-year spin-up to remove the effect of initial conditions. We also present a number of sensitivity simulations conducted at 4° x 5° horizontal resolution, which yields results very similar to the 2° x 2.5° resolution. The largest differences in the two resolutions occur over regions of biomass burning. Over these locations, the finer horizontal resolution produces 10 – 20% more PAN. The likely explanation is that vertical transport is faster at higher resolution because eddies are not averaged out. This was first shown by Wang et al. (2004) using a nested simulation for CO over Asia.

Emily Fischer 1/17/14 3:29 PM
Formatted: Font:Not Italic

Emily Fischer 1/17/14 3:29 PM
Formatted: Font:Italic

Throughout the paper we present results using 2008 GEOS-5 assimilated meteorology. However we have compared results using both GEOS-4 and GEOS-5 for 2006, the last year of overlap for these two meteorological datasets. The lifetime of PAN doubles for every 4 K decrease in temperature. PAN is also sensitive to biogenic emissions, lightning NO_x emissions and vertical transport (Labrador et al., 2005), parameters that also depend on the underlying meteorological field. We found that differences in the monthly mean PAN produced using different assimilated meteorological grids are substantial in some locations (< 100 pptv). Higher upper-tropospheric PAN mixing ratios over the tropical Pacific in GEOS-5 appear to be driven by slower convective overturning in GEOS-5 than GEOS-4. GEOS-4 agrees better with data from PEM-Tropics B (Maloney et al., 2001). The PEM-Tropics B dataset suggests very low (<50 pptv) PAN mixing ratios in the Pacific tropical UT. Differences between the simulated and observed O_3 profiles for the

PEM-Tropics B regions are consistent with the view that differences in vertical motion are driving the PAN differences. There are limited opportunities to chemically constrain convective overturning in data assimilation models. However, existing analyses suggest substantial differences between overturning rates derived from in situ measurements and those in GEOS-4 (Bertram et al., 2007). Mitoviski et al. (2012) assessed the impact of convection on O_3 in GEOS-Chem and found tropical upper tropospheric O_3 biases driven by the parameterized vertical transport in both GEOS-4 and GEOS-5.

3. Global PAN distribution

We used a large database of recent PAN observations from surface sites and airborne campaigns to evaluate the model, and these are presented in Table 2. For comparison to the model, we averaged the aircraft observations over the coherent regions in Figure 1. The measurements either relied on gas chromatography with electron capture detector (GC-ECD) (Flocke et al., 2005) or thermal decomposition chemical ionization mass spectrometry (TD-CIMS) (Zheng et al., 2011).

Figures 2 and 3 compare the observed global distribution of PAN to that simulated by GEOS-Chem. Mean observations from the studies compiled in Table 2 are shown as filled circles. Model fields are background contours. Full vertical profiles (median and mean) for the aircraft campaigns and seasonal cycles for several European mountain top datasets are in the supplementary materials. We compare model output from 2008 to observations collected over many years. Interannual variability in the model is smaller than other sources of error. There are relatively few in situ observations that can be used to assess interannual variability in PAN (Bottenheim et al., 1994). Observations at Mount Bachelor, (Oregon, USA) indicate interannual variability of 20% during the spring

317 maximum (Fischer et al., 2011). Recent trends in PAN in many regions of the atmosphere
318 are also hard to assess given a paucity of consistent data (Parrish et al., 2004). As shown
319 later PAN is highly sensitive to NO_x and NMVOC emissions, both of which have changed
320 considerably in some regions (Pollack et al., 2013).

321 Figure 2 indicates that spring and summer northern hemisphere average PAN
322 abundances below 6 km are comparable over polluted continental region. The northern
323 hemisphere springtime maximum, previously attributed to photochemical production at a
324 time when PAN has a long thermal lifetime (Penkett and Brice, 1986; Brice et al., 1988), is
325 primarily a feature of remote air. Long term PAN measurements from the
326 Hohenpeissenberg and Schauinsland European mountaintop observatories, both primarily
327 within the atmospheric boundary layer, show either spring or summer maxima depending on
328 the year (Supplementary Figure 2). Pandey Deolal et al. (2013) found that the PAN spring
329 maximum at the Jungfraujoch is mainly attributable to airmasses advected from the polluted
330 European boundary layer, and PAN formation in the free troposphere does not play a
331 dominant role. Both the model and surface observations indicate that the springtime
332 maximum is pronounced over the Arctic, and this has previously been attributed to transport
333 of northern mid-latitudes pollution (Moxim et al., 1996). We find that springtime fires in
334 Russia and China also contribute to this feature, and this is discussed later in the context of
335 our sensitivity simulations.

336 Successful simulation of PAN in Asian outflow is contingent on the inclusion of
337 emissions of aromatic species. These account for 30% of the PAN in that region in the
338 model. Even with the addition of aromatics, the model is biased low for this region. This
339 could suggest missing NMVOC emissions in China, as suggested by Fu et al. (2007) or

340 unrealistically low PA radical yields from aromatics in the chemical scheme. The model
341 largely reproduces the average vertical profiles observed during TRACE-P (see vertical
342 profiles in Supplementary Figure 1), but these were collected in 2001 and the model output
343 is for 2008. Chinese NO_x and NMVOCs emissions have increased by more than 55% and
344 29% over this period respectively (Zhang et al., 2009; Zhang et al., 2007b).

345 PAN is also sensitive to the parameterization of the uptake of the hydroperoxyl
346 radical (HO_2) by aerosols. Recent work (Mao et al., 2013a) suggests that the reactive
347 uptake of HO_2 is a much more efficient sink of HO_x than previously thought (Thornton et al.,
348 2008) and implemented in the version of GEOS-Chem used here. We tested the impact of
349 more efficient uptake of HO_2 by aerosols on PAN by setting the reactive uptake coefficient
350 of HO_2 to 1 and eliminating conversion of HO_2 to H_2O_2 on aerosols. We found that the
351 faster uptake of HO_2 drastically reduced (50%) springtime PAN over East Asia. The faster
352 uptake produces springtime PAN outflow in the model that is inconsistent with observations
353 in that region, and would imply a large missing source of PAN.

354 Though the differences are smaller, PAN observations from European mountain top
355 sites also suggest missing PAN sources there. These PAN observations have not been used
356 to justify emissions changes as observations from both Zugspitze (2658 m) and
357 Jungfraujoch (3580 m) reflect terrain-induced injections of PAN rich boundary layer air
358 (Zanis et al., 2007; Zellweger et al., 2000; Carpenter et al., 2000; Zanis et al., 2003; Pandey
359 Deolal et al., 2013), and this transport scale is not captured in the model. However, Figure 3
360 indicates that the observations are also higher than the model output below the altitude of
361 the measurements.

362 In northern hemisphere summer, both the model and observations show a strong

363 contrast between high concentrations over source continents and adjacent oceans (Figure 3),
364 reflecting the short lifetime of PAN against thermal decomposition. PAN concentrations in
365 the model are generally higher aloft, consistent with INTEX-A aircraft observations over the
366 eastern US (90 °W – 45 °W, Panel 3, Figure 3) and measurements from the Azores (Val
367 Martin et al., 2008), reflecting the longer PAN lifetime. The INTEX-A observations
368 indicate that PAN mixing ratios begin to decrease with altitude above 8 km over the
369 northeastern U.S. and the western Atlantic, but not over the southeastern U.S. where
370 lightning and convection support PAN production aloft (Hudman et al., 2007).

371 The lowest three panels of Figure 3 show that outside of winter months, there is a
372 reservoir of 200 – 400 pptv PAN between 5 – 8 km over northern mid-latitudes. A similar
373 PAN reservoir aloft has also been observed over the Arctic during aircraft campaigns in
374 spring and summer (Singh et al., 1994). PAN can be 80 – 90% of total NO_y in the cold
375 arctic atmosphere (Atlas et al., 2003; Jaffe et al., 1997; Bottenheim et al., 1986). Liang et al.
376 (2011) note that the 2008 ARCTAS PAN observations are not notably different from either
377 the 1988 ABLE or 2000 TOPSE observations, despite dramatic changes to NO_X emissions
378 in the major anthropogenic source regions. In the upper troposphere, northern hemisphere
379 PAN mixing ratios peak in summer, with contributions from anthropogenic sources,
380 biomass burning and lightning. This summertime upper tropospheric maximum is
381 consistent with MIPAS retrievals for 300 – 150 hPa which indicate the highest Northern
382 Hemisphere PAN concentrations in August and the lowest PAN from October to January
383 (Moore and Remedios, 2010).

384 The Polarstern Cruise data from Germany to South Africa in summer reveals a sharp
385 meridional gradient with mixing ratios dropping below the detection limit (25 pptv) outside

Emily Fischer 1/8/14 11:18 PM
Deleted: As we see in Figure S1, t

387 northern mid-latitudes (Figure 2) (Jacobi et al., 1999). The meridional gradient is much less
388 defined in the free troposphere, reflecting biogenic and fire contributions in the southern
389 tropics with efficient convective lofting (Figure 2).

390 We see from the SON seasonal mean plots in Figure 2 that the southern hemisphere
391 features a spring PAN maximum in the upper troposphere, similar to the remote northern
392 extra-tropics. Moore and Remedios (2010) observed a spring PAN maximum in the upper
393 troposphere at 0-35°S from MIPAS retrievals and attributed it to seasonal biomass burning
394 over Central Africa. Moxim et al. (1999) also simulated the southern hemisphere springtime
395 free tropospheric PAN maximum, but suggested that it is driven by convective transport
396 rapidly mixing PAN upward from continental surface production regions. As discussed
397 below, our model suggests that much of the PAN in the austral free troposphere is due to
398 continental convective injection of biogenic NMVOCs together with the lightning NO_x
399 source.

400 **4. Contributions of different NMVOCs to PAN formation**

401 PAN depends on NMVOCs and NO_x in nonlinear ways. To diagnose this
402 dependence and identify the most critical precursor, we conducted two sensitivity studies
403 where NO_x and NMVOC emissions were separately reduced by 20% across all sectors. The
404 results are presented in Figure 4. We see that PAN concentration depends in general more
405 strongly on NMVOC than NO_x emissions. Exceptions are fire-dominated regions at
406 northern high latitudes, reflecting the very low NO_x/NMVOCs emission ratio from fires.
407 This result is also partially an artifact of partitioning 40% of GFED fire NO_x emissions
408 directly to PAN. A remarkable result is that PAN responds supra-linearly to NMVOC

409 emissions in many locations, with the strongest effect over the North Pacific in spring and
410 over the Arctic in summer. In both of these regions PAN is a principal source of NO_x
411 (Singh et al., 1992; Zhang et al., 2008), so that reducing PAN causes decreases in O_3, in turn
412 decreasing the $[NO_2]/[NO]$ ratio and thus reducing the effective lifetime of PAN. This
413 chemical feedback amplifies the sensitivity of PAN to NMVOC emission changes. Another
414 chemical feedback in source regions is that reducing NMVOC emissions increases the
415 concentration of OH and hence the conversion of NO_x to nitric acid.

416 In order to understand the contributions of different NMVOC precursors to PAN
417 formation, we conducted 14 sensitivity simulations where the emissions of each precursor in
418 the leftmost column of Table 1 were turned off individually. The change in the total burden
419 of PAN was compared to a standard simulation with all emissions switched on. In the case
420 of isoprene where the effect is large, we reduced emissions by 20% (and multiplied the
421 change by 5) in order to minimize non-linear effects. Figure 5 presents a schematic of the
422 relative contributions of individual NMVOCs to global PAN formation through the major
423 carbonyl species (acetaldehyde, acetone, methylglyoxal) serving as precursors of PAN
424 (reactions (2) – (4)). The absolute contributions are in Table 1. Anthropogenic, biogenic
425 and biomass burning emissions make significant contributions to all three of the most
426 important immediate PAN precursors (acetaldehyde, acetone, and methylglyoxal). We track
427 PA radical formation via four different chemical pathways, from acetaldehyde, acetone,
428 methylglyoxal and via all other intermediate species. The bottom pie chart in Figure 5
429 summarizes the relative importance of these four pathways for global annual total PA
430 radical production.

431 Figure 6 summarizes the geographical distribution of annual total PA radical

production for the lower, mid- and upper troposphere. PA production is strongest in NMVOC source regions, propagating to the free troposphere in the tropics through deep convection. The patterns in Figure 6 reflect the dominant sources and lifetime for each PA radical precursor: mean lifetimes 1-2 hours for methylglyoxal, 0.8 days for acetaldehyde and 14 days for acetone. The bottom row of Figure 6 shows total PA radical production from other pathways, mainly via isoprene and monoterpene oxidation intermediates including methylvinyl ketone and methacrolein. These latter species contribute to PA radical formation predominantly via photolysis. We traced PA radical formation via these species together with all other intermediates.

Figure 5 and Figure 6 reveal that acetaldehyde is the most important PA radical precursor globally, responsible for ~40% of total PA radical production at all altitudes. Photochemical production is the dominant source of acetaldehyde, with large contributions from both biogenic and anthropogenic primary emissions (Figure 5). There is also PA production from acetaldehyde in the marine boundary layer, partially reflecting the ocean acetaldehyde source (Millet et al., 2010). The alkanes, $>C_2$ alkenes and ethanol all have high molar yields for acetaldehyde (Table 1). Though most originate over continents, the lifetimes of the primary precursors of acetaldehyde range from hours (isoprene) to months (ethane). Thus there is significant production of the PA radical from acetaldehyde at all altitudes over both continental regions and the downwind oceans (Millet et al., 2010).

Based on global simulations with and without acetone, Singh et al. (1995) estimated that up to 50% of observed PAN in the mid-upper troposphere could be formed from acetone. However, they assumed a photolysis rate for acetone now known to be too high. Using a similar approach and the acetone budget from Fischer et al. (2012), we find that the

Emily Fischer 1/12/14 11:20 AM
Deleted: that

456 contribution of acetone to PAN is 25% in the upper troposphere over the northern
457 hemisphere during summer and less under other conditions. Acetone is the most important
458 PA precursor only in the most remote regions of the upper troposphere.

459 Isoprene and monoterpenes are also important precursors for PAN formation through
460 methylgyoxal and other intermediates. Due to relatively short lifetimes, their role is largest
461 in continental boundary layers (Figure 6). von Kuhlmann et al. (2004) showed that PAN
462 formation in models is highly sensitive to the treatment of isoprene chemistry, and there
463 have been a number of more recent advances regarding the oxidation chemistry of isoprene
464 (Lelieveld et al., 2008; Paulot et al., 2009b; Peeters et al., 2009; Mao et al., 2012). There
465 are also ongoing efforts to determine appropriate yields for methylglyoxal and other
466 important intermediates under the high NO_x conditions most relevant for PAN formation
467 (Galloway et al., 2011). Implementation of the Paulot et al. (2009a,b) oxidation scheme in
468 GEOS-Chem improves the simulation of summertime observations over the southeastern
469 U.S (Mao et al., 2013b). It also substantially increases surface PAN mixing ratios over the
470 Amazon and Central Africa, where there is very little observational data (Angelo, 2012). In
471 these regions surface PAN increases by 100 – 300 pptv with the Paulot et al. (2009a,b)
472 scheme, but the impact is more modest above the boundary layer, generally less than 50
473 pptv. In the model, most of the free tropospheric PAN in convective regions is produced
474 above the boundary layer.

475 **5. Contributions from Different Source Types to PAN formation**

476 Figure 7 presents the sensitivity of PAN concentrations to different emission types,
477 as diagnosed by the relative decrease in a sensitivity simulation with that emission type shut

478 off. Contributions do not add up to 100% because of non-linearity.

479 During northern hemisphere spring, shutting off anthropogenic emissions decreases
480 the integrated PAN burden by ~50%. Alkanes are the most important class of
481 anthropogenic NMVOC precursors for PAN in northern mid-latitudes. Their role is more
482 important in spring when NMVOC emissions from the biosphere are smaller. In spring, the
483 time of the surface PAN maximum, biogenic and anthropogenic NMVOCs species each
484 support ~50% of the PAN burden.

485 Though most biomass burning occurs primarily in the tropics, the effect of fires on
486 PAN appears to be largest at northern latitudes. Shutting off emissions from springtime fires
487 located in Russia and China decreases the hemispheric burden by ~25%, but the decrease in
488 PAN mixing ratios is 30 – 40 % at high latitudes. These springtime fires, which exhibit
489 strong variability in magnitude and location, contribute to the observed spring PAN
490 maximum. Russian fires likely accentuated this feature in April 2008, an unusually strong
491 fire season (Vivchar, 2010; Warneke et al., 2009; Warneke et al., 2010). PAN in fire
492 plumes from the Russian Federation was shown to support efficient O_3 production over the
493 northeast Pacific during April 2008 (Fischer et al., 2010). Enhancements in O_3 of up to 20
494 ppbv were observed during this time from Alaska to California (Oltmans et al., 2010).
495 Spring 2008 was an extreme burning year, but Macdonald et al. (2011) also attribute
496 elevated monthly mean O_3 concentrations at Whistler Mountain, BC in fall 2002 and spring
497 2003 to fires in the Russian Federation.

498 As stated earlier, the treatment of PAN formation in fires plays an important role in
499 determining the global impact of this PAN source. Past model studies have found that

reproducing observed free tropospheric CO and O_3 downwind from boreal fires requires injecting a fraction of the emissions above the boundary layer (Leung et al., 2007; Turquety et al., 2007; Generoso et al., 2007; Colarco et al., 2004). Tereszchuk et al. (2013) show that PAN in the upper troposphere at high latitudes is mainly from large boreal fires in summer. Emitting a fraction of the smoke above the boundary layer is an important model update that improves the simulation of the 2 - 6 km PAN reservoir at high latitudes. The fraction of NO_x in the springtime Russian fires that is immediately partitioned to PAN also has a large impact on springtime PAN over high latitudes because PAN has a long lifetime during this season. The combination of model updates chosen here best reproduces the evolution of the springtime PAN profile as observed during TOPSE (Wang et al., 2003). Specifically, PAN remains relatively constant (150 – 200 pptv) with altitude in February and March, and the 2 - 6 km PAN reservoir forms in April. Springtime PAN in the model is acutely sensitive to the amount of NO_x that is immediately partitioned to PAN in fires. Given that O_3 production in the Arctic lower troposphere is sensitive to the abundance of PAN (Walker et al., 2012; Beine et al., 1997), more work is warranted to determine the best way to incorporate the chemistry that rapidly produces PAN in fires.

We find that biogenic species drive PAN production in summer and fall. From June to October, shutting off biogenic emissions decreases the northern hemisphere integrated PAN burden by ~75 %. In summer, the contribution to PAN from other biogenic NMVOCs (terpenes, acetone, acetaldehyde, ethanol and higher alkenes) is ~50 % that of isoprene. Consistent with our analysis, Roberts et al. (2006) estimated that the isoprene contribution to PAN formation is 1.6 to 4 times larger than the anthropogenic NMVOC contribution in the northeastern U.S. in summer.

The austral spring mid-to-upper tropospheric PAN maximum (>400 pptv) spanning the Atlantic (Figure 2) is also apparent in MIPAS PAN retrievals (Glatthor et al., 2007; Moore and Remedios, 2010; Wiegele et al., 2012). Figure 7 shows that this feature is more sensitive to emissions of NO_x from lightning than emissions from either biomass burning or anthropogenic sources. Biomass burning takes place from July to October in the part of Africa located in the southern hemisphere. Singh et al. (1996a) found that PAN correlated with tracers of biomass combustion in the eastern South Atlantic in the lower and middle troposphere, but not in the upper troposphere. To explain observed NO_x at higher altitudes, they had to invoke a large contribution from lightning (Smyth et al., 1996). Our simulation reproduces the TRACE-A vertical PAN profiles for the South Atlantic (Supplementary Figure 1, Panels 43-45) and the correlation between PAN and CO (not shown). We find that fires are responsible for approximately 30% of the PAN over the tropical Atlantic between 2 and 4 km. Above 6 km, the contribution from fires is small. In the upper troposphere, the oxidation of biogenic NMVOCs (lifted by convection (Murphy et al., 2010; Bechara et al., 2010; Warneke et al., 2001)) in the presence of lightning NO_x is a large source of PAN (Tie et al., 2001; Labrador et al., 2005). Compared to the previous version of GEOS-Chem, the sensitivity of upper tropospheric PAN to lightning is reduced by 30%. We attribute this change to increased OH in the boundary layer through the use of the Paulot et al. (2009a, b) isoprene scheme, that reduces the amount of NMVOC injected into the free troposphere (Paulot et al., 2012). Boundary layer and upper tropospheric chemistry in the tropics are tightly coupled (Paulot et al., 2012). Hence the simulation of upper tropospheric PAN is sensitive to the representation of boundary layer chemistry, which remains very uncertain (Hewitt et al., 2010).

6. Conclusions

We utilized a worldwide collection of observations to improve a global simulation of PAN in the GEOS-Chem model. This new simulation, which includes an improved representation of numerous NMVOCs and a different treatment of biomass burning emissions, affords the opportunity to understand the factors driving the PAN distribution on the global scale.

1. We find that PAN is generally more sensitive to NMVOC emissions than NO_x emissions. In many regions of the atmosphere, changes to NMVOC emissions produce a supra-linear change in PAN through feedbacks to remote NO_x and O_3 budgets. A different mixture of NMVOCs supports PAN formation in each region and season. Considerable improvement of the PAN simulation for the Asian outflow region is achieved by including aromatics. Our results stress the need for global CTMs, which can yield different results for PAN (Singh et al., 2007), to include and evaluate budgets for many NMVOCs that are routinely ignored.

2. In order to reproduce the observed PAN reservoir at 3-6 km over high northern latitudes, we have changed the way emissions from fires are incorporated into the model. We increased the simulated PAN reservoir over high latitudes by 1) adding biomass burning emissions of shorter lived NMVOCs (monoterpenes, aromatics), 2) emitting a fraction of the biomass burning NO_x directly as PAN (Alvarado et al., 2010), 3) emitting a portion of the smoke above the boundary layer, 4) updating the emission factors for NMVOCs and NO_x (Akagi et al., 2011), and increasing emissions to account for undetected small fires at high latitudes (Kaiser et al., 2012). We find that PAN over the Arctic is very sensitive to fires, and particularly sensitive to the amount of NO_x that is immediately partitioned to PAN in

568 fires and to the altitude of the emissions. Given that O_3 production in the Arctic lower
569 troposphere is very sensitive to NO_x abundance (Stroud et al., 2004; Walker et al., 2012),
570 more work is warranted to determine the best way to incorporate the plume chemistry that
571 rapidly produces PAN into CTMs.

572 3. The principal carbonyl precursors of PAN are acetaldehyde (44% of the global source),
573 methylglyoxal (30%) and acetone (7%). Acetaldehyde is produced by a large suite of
574 NMVOCs and also directly emitted. Methylglyoxal is mostly from isoprene. Isoprene
575 oxidation products, other than methylglyoxal, are also significant. With updated (lower)
576 photolysis yields, acetone is a substantially less important pathway for PAN formation than
577 previously thought (Singh et al., 1995).

578 4. Isoprene accounts for 37% of the global PAN burden. Many other NMVOC emissions
579 contribute to the balance, with no single species contributing more than 10% (Table 1). At
580 northern hemisphere mid-latitudes, alkanes contribute to a third of PAN formation during
581 the springtime maximum.

582 5. A springtime upper troposphere PAN maximum across the tropical Atlantic is the major
583 feature of the southern hemisphere PAN distribution. Lightning is the most important NO_x
584 source for PAN formation in this region of the atmosphere. A cascade of isoprene oxidation
585 products, delivered to the upper troposphere by deep convection, provides the PA radical
586 source. This finding is sensitive to the description of boundary layer chemistry under low
587 NO_x conditions.

588 The work presented here has increased confidence in our ability to simulate the observed
589 distribution of PAN within the GEOS-Chem CTM. In a follow-up paper we will examine

590 the importance of PAN in affecting global tropospheric O_3 and OH, and the implications for
591 intercontinental transport of pollution, the oxidizing power of the atmosphere, and climate
592 forcing.

593 **Acknowledgements**

594 This work was supported by the NASA Atmospheric Composition Modeling and Analysis
595 Program. Support for Emily V. Fischer was provided by the NOAA Climate and Global
596 Change Postdoctoral Fellowship Program, administered by UCAR, and by a Harvard
597 University Center for the Environment Postdoctoral Fellowship. The contribution of PAN
598 data from the GAW Global Station Hohenbeissenberg by Stefan Gilge, German
599 Meteorological Service, is greatly acknowledged. The contribution of PAN data from the
600 Jungfraujoch Mountain Site by Christoph Zellweger (EMPA) is greatly acknowledged. We
601 thank Hiroshi Tanimoto for providing the data from Rishiri, Japan. Pico PAN data were
602 collected under the leadership of Richard Honrath with funding from the National Science
603 Foundation grant ATM-0720955. Funding for the analysis of the Pico PAN measurements
604 by Katja Dzepina, Jim Roberts and Lynn Mazzoleni was provided by the National Science
605 Foundation through grant AGS-1110059. We also appreciate the contribution of
606 unpublished PAN data from the Thompson Farm AIRMAP Site by Ryan Chartier. Finally,
607 we thank Martin Steinbacher and Jim Roberts for helpful comments on the manuscript.

608

References

Akagi, S. K., Yokelson, R. J., Wiedinmyer, C., Alvarado, M. J., Reid, J. S., Karl, T., Crounse, J. D., and Wennberg, P. O.: Emission factors for open and domestic biomass burning for use in atmospheric models, Atmos. Chem. Phys., 11, 4039-4072, 10.5194/acp-11-4039-2011, 2011.

Alvarado, M. J., Logan, J. A., Mao, J., Apel, E., Riemer, D., Blake, D., Cohen, R. C., Min, K. E., Perring, A. E., Browne, E. C., Wooldridge, P. J., Diskin, G. S., Sachse, G. W., Fuelberg, H., Sessions, W. R., Harrigan, D. L., Huey, G., Liao, J., Case-Hanks, A., Jimenez, J. L., Cubison, M. J., Vay, S. A., Weinheimer, A. J., Knapp, D. J., Montzka, D. D., Flocke, F. M., Pollack, I. B., Wennberg, P. O., Kurten, A., Crounse, J., Clair, J. M. S., Wisthaler, A., Mikoviny, T., Yantosca, R. M., Carouge, C. C., and Le Sager, P.: Nitrogen oxides and PAN in plumes from boreal fires during ARCTAS-B and their impact on ozone: an integrated analysis of aircraft and satellite observations, Atmos. Chem. Phys., 10, 9739-9760, 10.5194/acp-10-9739-2010, 2010.

Ammann, M., Cox, R. A., Crowley, J. N., Jenkin, M. E., Mellouki, A., Rossi, M. J., Troe, J., and Wallington, T. J.: Evaluated kinetic and photochemical data for atmospheric chemistry: Volume VI – heterogeneous reactions with liquid substrates, Atmos. Chem. Phys., 13, 8045-8228, doi:10.5194/acp-13-8045-2013, 2013.

Angelo, C.: Amazon fire analysis hits new heights, Nature News, 10.1038/nature.2012.11467, 2012.

Atkinson, R. and J. Arey: Gas-phase tropospheric chemistry of biogenic volatile organic compounds: a review, Atmospheric Environment, 37 Supplement No. 2, S197-S219, 2003.

Atlas, E. L., Ridley, B. A., and Cantrell, C. A.: The Tropospheric Ozone Production about the Spring Equinox (TOPSE) Experiment: Introduction, J. Geophys. Res., 108, 8353, 10.1029/2002jd003172, 2003.

Balzani Loov, J. M., Henne, S., Legreid, G., Staehelin, J., Reimann, S., Prevut, A. S. H., Steinbacher, M., and Vollmer, M. K.: Estimation of background concentrations of trace gases at the Swiss Alpine site Jungfraujoch (3580 m asl), J. Geophys. Res., 113, D22305, 10.1029/2007jd009751, 2008.

Barletta, B., Meinardi, S., Simpson, I. J., Sherwood Rowland, F., Chan, C.-Y., Wang, X., Zou, S., Chan, L. Y., and Blake, D. R.: Ambient halocarbon mixing ratios in 45 Chinese cities, Atmos. Env., 40, 7706-7719, 10.1016/j.atmosenv.2006.08.039, 2006.

Bechara, J., Borbon, A., Jambert, C., Colomb, A., and Perros, P. E.: Evidence of the impact of deep convection on reactive Volatile Organic Compounds in the upper tropical troposphere during the AMMA experiment in West Africa, Atmos. Chem. Phys., 10, 10321-10334, 10.5194/acp-10-10321-2010, 2010.

Emily Fischer 1/17/14 3:34 PM
Formatted: Font:12 pt, Not Italic

Emily Fischer 1/12/14 8:13 PM
Formatted: Space After: 0 pt, No widow/orphan control, Don't adjust space between Latin and Asian text, Don't adjust space between Asian text and numbers

Emily Fischer 1/12/14 8:13 PM
Formatted: Font:10 pt, Italic, Check spelling and grammar

Beine, H., Jaffe, D., Herring, J., Kelley, J., Krognes, T., and Stordal, F.: High-Latitude Springtime Photochemistry. Part I: NO_x, PAN and Ozone Relationships, J. Atmos. Chem., 27, 127-153, 10.1023/a:1005869900567, 1997.

Beine, H. J., Jaffe, D. A., Blake, D. R., Atlas, E., and Harris, J.: Measurements of PAN, alkyl nitrates, ozone, and hydrocarbons during spring in interior Alaska, J. Geophys. Res., 101, 12613-12619, 10.1029/96jd00342, 1996.

Beine, H. J., and Krognes, T.: The seasonal cycle of peroxyacetyl nitrate (PAN) in the European Arctic, Atmos. Env., 34, 933-940, 10.1016/s1352-2310(99)00288-5, 2000.

Bertram, T. H., Perring, A. E., Wooldridge, P. J., Crounse, J. D., Kwan, A. J., Wennberg, P. O., Scheuer, E., Dibb, J., Avery, M., Sachse, G., Vay, S. A., Crawford, J. H., McNaughton, C. S., Clarke, A., Pickering, K. E., Fuelberg, H., Huey, G., Blake, D. R., Singh, H. B., Hall, S. R., Shetter, R. E., Fried, A., Heikes, B. G., and Cohen, R. C.: Direct Measurements of the Convective Recycling of the Upper Troposphere, Science, 315, 816-820, 10.1126/science.1134548, 2007.

Bertram, T. H., Perring, A. E., Wooldridge, P. J., Dibb, J., Avery, M. A., and Cohen, R. C.: On the export of reactive nitrogen from Asia: NOx partitioning and effects on ozone, Atmos. Chem. Phys., 13, 4617-4630, 10.5194/acp-13-4617-2013, 2013.

Bey, I., Jacob, D. J., Yantosca, R. M., Logan, J. A., Field, B. D., Fiore, A. M., Li, Q., Liu, H. Y., Mickley, L. J., and Schultz, M. G.: Global modeling of tropospheric chemistry with assimilated meteorology: Model description and evaluation, J. Geophys. Res., 106, 23073-23095, 10.1029/2001jd000807, 2001.

Bloss, C., Wagner, V., Jenkin, M. E., Volkamer, R., Bloss, W. J., Lee, J. D., Heard, D. E., Wirtz, K., Martin-Reviejo, M., Rea, G., Wenger, J. C., and Pilling, M. J.: Development of a detailed chemical mechanism (MCMv3.1) for the atmospheric oxidation of aromatic hydrocarbons, Atmos. Chem. Phys., 5, 641-664, doi:10.5194/acp-5-641-2005, 2005.

Bottenheim, J. W., Gallant, A. G., and Brice, K. A.: Measurements of NO_Y species and O_3 at 82° N latitude, Geophys. Res. Lett, 13, 113-116, 10.1029/GL013i002p00113, 1986.

Bottenheim, J. W., Sirois, A., Brice, K. A., and Gallant, A. J.: Five years of continuous observations of PAN and ozone at a rural location in eastern Canada, J. Geophys. Res, 99, 5333-5352, 10.1029/93jd02716, 1994.

Brice, K. A., Bottenheim, J. W., Anlauf, K. G., and Wiebe, H. A.: Long-term measurements of atmospheric peroxyacetylnitrate (PAN) at rural sites in Ontario and Nova Scotia; seasonal variations and long-range transport, Tellus B, Vol 40, 1988.

Bridier, I., Caralp, F., Loirat, H., Lesclaux, R., Veyret, B., Becker, K. H., Reimer, A., and Zabel, F.: Kinetic and theoretical studies of the reactions of acetylperoxy + nitrogen dioxide + M <--> acetyl peroxynitrate + M between 248 and 393 K and between 30 and 760 torr, J. Phys.Chem., 95, 3594-3600, 10.1021/j100162a031, 1991.

684 Carpenter, L. J., Green, T. J., Mills, G. P., Bauguitte, S., Penkett, S. A., Zanis, P.,
685 Schuepbach, E., Schmidbauer, N., Monks, P. S., and Zellweger, C.: Oxidized nitrogen and
686 ozone production efficiencies in the springtime free troposphere over the Alps, J. Geophys.
687 Res., 105, 14547-14559, 10.1029/2000jd900002, 2000.

688 Colarco, P. R., Schoeberl, M. R., Doddridge, B. G., Marufu, L. T., Torres, O., and Welton,
689 E. J.: Transport of smoke from Canadian forest fires to the surface near Washington, D.C.:
690 Injection height, entrainment, and optical properties, J. Geophys. Res., 109, D06203,
691 10.1029/2003jd004248, 2004.

692 Dassau, T. M., Shepson, P. B., Bottenheim, J. W., and Ford, K. M.: Peroxyacetyl nitrate
693 photochemistry and interactions with the Arctic surface, J. Geophys. Res., 109, D18302,
694 10.1029/2004jd004562, 2004.

695 Fischer, E. V., Jaffe, D. A., Reidmiller, D. R., and Jaegle, L.: Meteorological controls on
696 observed peroxyacetyl nitrate at Mount Bachelor during the spring of 2008, J. Geophys.
697 Res., 115, D03302, 10.1029/2009jd012776, 2010.

698 Fischer, E. V., Jaffe, D. A., and Weatherhead, E. C.: Free tropospheric peroxyacetyl nitrate
699 (PAN) and ozone at Mount Bachelor: causes of variability and timescale for trend detection,
700 Atmos. Chem. Phys. 11, 5641-5654, 10.5194/acp-11-5641-2011, 2011.

701 Fischer, E. V., Jacob, D. J., Millet, D. B., Yantosca, R. M., and Mao, J.: The role of the
702 ocean in the global atmospheric budget of acetone, Geophys. Res. Lett., 39, L01807,
703 10.1029/2011gl050086, 2012.

704 Flocke, F., Weinheimer, A., Swanson, A., Roberts, J., Schmitt, R., and Shertz, S.: On the
705 Measurement of PANs by Gas Chromatography and Electron Capture Detection, J. Atmos.
706 Chem., 52, 19-43, 10.1007/s10874-005-6772-0, 2005.

707 Ford, K. M., Campbell, B. M., Shepson, P. B., Bertman, S. B., Honrath, R. E., Peterson, M.,
708 and Dibb, J. E.: Studies of Peroxyacetyl nitrate (PAN) and its interaction with the snowpack
709 at Summit, Greenland, J. Geophys. Res., 107, 4102, 10.1029/2001jd000547, 2002.

710 Fu, T.-M., Jacob, D. J., Palmer, P. I., Chance, K., Wang, Y. X., Barletta, B., Blake, D. R.,
711 Stanton, J. C., and Pilling, M. J.: Space-based formaldehyde measurements as constraints on
712 volatile organic compound emissions in east and south Asia and implications for ozone, J.
713 Geophys. Res., 112, D06312, 10.1029/2006jd007853, 2007.

714 Galloway, M. M., Huisman, A. J., Yee, L. D., Chan, A. W. H., Loza, C. L., Seinfeld, J. H.,
715 and Keutsch, F. N.: Yields of oxidized volatile organic compounds during the OH radical
716 initiated oxidation of isoprene, methyl vinyl ketone, and methacrolein under high-NO_x
717 conditions, Atmos. Chem. Phys. 11, 10779-10790, 10.5194/acp-11-10779-2011, 2011.

718 Generoso, S., Bey, I., Attié, J.-L., and Bréon, F.-M.: A satellite- and model-based
719 assessment of the 2003 Russian fires: Impact on the Arctic region, J. Geophys. Res., 112,
720 D15302, 10.1029/2006jd008344, 2007.

721 Glatthor, N., von Clarmann, T., Fischer, H., Funke, B., Grabowski, U., Hopfner, M.,
722 Kellmann, S., Kiefer, M., Linden, A., Milz, M., Steck, T., and Stiller, G. P.: Global
723 peroxyacetyl nitrate (PAN) retrieval in the upper troposphere from limb emission spectra of
724 the Michelson Interferometer for Passive Atmospheric Sounding (MIPAS), Atmos. Chem.
725 Phys., 7, 2775-2787, 10.5194/acp-7-2775-2007, 2007.

726 Goliff, W. S., Stockwell, W. R., and Lawson, C. V.: The regional atmospheric chemistry
727 mechanism, version 2, Atmos. Env., 68, 174-185,
728 http://dx.doi.org/10.1016/j.atmosenv.2012.11.038, 2013.

729 Grosjean, D., Grosjean, E., and Williams, E. L.: Thermal Decomposition of PAN, PPN and
730 Vinyl-PAN, Air & Waste, 44, 391-396, 10.1080/1073161x.1994.10467260, 1994.

731 Guenther, A., Karl, T., Harley, P., Wiedinmyer, C., Palmer, P. I., and Geron, C.: Estimates
732 of global terrestrial isoprene emissions using MEGAN (Model of Emissions of Gases and
733 Aerosols from Nature), Atmos. Chem. Phys., 6, 3181-3210, 10.5194/acp-6-3181-2006, 2006.

734 Guo, J., A. Tilgner, C. Yeung, Z. Wang, P. K. K. Louie, C. W. Y. Luk, Z. Xu, C. Yuan, Y.
735 Gao, S. Poon, H. Herrmann, S. Lee, K. S. Lam, and T. Wang, Atmospheric Peroxides in a
736 Polluted Subtropical Environment: Seasonal Variation, Sources and Sinks, and
737 Importance of Heterogeneous Processes, Environmental Science & Technology,
738 10.1021/es403229x, 2013.

739 Hewitt, C. N., Lee, J. D., MacKenzie, A. R., Barkley, M. P., Carslaw, N., Carver, G. D.,
740 Chappell, N. A., Coe, H., Collier, C., Commane, R., Davies, F., Davison, B., DiCarlo, P., Di
741 Marco, C. F., Dorsey, J. R., Edwards, P. M., Evans, M. J., Fowler, D., Furneaux, K. L.,
742 Gallagher, M., Guenther, A., Heard, D. E., Helfter, C., Hopkins, J., Ingham, T., Irwin, M.,
743 Jones, C., Karunaharan, A., Langford, B., Lewis, A. C., Lim, S. F., MacDonald, S. M.,
744 Mahajan, A. S., Malpass, S., McFiggans, G., Mills, G., Misztal, P., Moller, S., Monks, P. S.,
745 Nemitz, E., Nicolas-Perea, V., Oetjen, H., Oram, D. E., Palmer, P. I., Phillips, G. J., Pike, R.,
746 Plane, J. M. C., Pugh, T., Pyle, J. A., Reeves, C. E., Robinson, N. H., Stewart, D., Stone, D.,
747 Whalley, L. K., and Yin, X.: Overview: oxidant and particle photochemical processes above
748 a south-east Asian tropical rainforest (the OP3 project): introduction, rationale, location
749 characteristics and tools, Atmos. Chem. Phys., 10, 169-199, 10.5194/acp-10-169-2010, 2010.

750 Horowitz, L. W., Liang, J., Gardner, G. M., and Jacob, D. J.: Export of reactive nitrogen
751 from North America during summertime: Sensitivity to hydrocarbon chemistry, J. Geophys.
752 Res, 103, 13451-13476, 10.1029/97jd03142, 1998.

753 Hudman, R. C., Jacob, D. J., Cooper, O. R., Evans, M. J., Heald, C. L., Park, R. J.,
754 Fehsenfeld, F., Flocke, F., Holloway, J., Hübler, G., Kita, K., Koike, M., Kondo, Y.,
755 Neuman, A., Nowak, J., Oltmans, S., Parrish, D., Roberts, J. M., and Ryerson, T.: Ozone
756 production in transpacific Asian pollution plumes and implications for ozone air quality in
757 California, J. Geophys. Res, 109, n/a-n/a, 10.1029/2004jd004974, 2004.

758 Hudman, R. C., Jacob, D. J., Turquety, S., Leibensperger, E. M., Murray, L. T., Wu, S.,
759 Gilliland, A. B., Avery, M., Bertram, T. H., Brune, W., Cohen, R. C., Dibb, J. E., Flocke, F.
760 M., Fried, A., Holloway, J., Neuman, J. A., Orville, R., Perring, A., Ren, X., Sachse, G. W.,

761 Singh, H. B., Swanson, A., and Wooldridge, P. J.: Surface and lightning sources of nitrogen
762 oxides over the United States: Magnitudes, chemical evolution, and outflow, J. Geophys.
763 Res., 112, D12S05, 10.1029/2006jd007912, 2007.

764 Ito, A., Sillman, S., and Penner, J. E.: Effects of additional nonmethane volatile organic
765 compounds, organic nitrates, and direct emissions of oxygenated organic species on global
766 tropospheric chemistry, J. Geophys. Res., 112, D06309, 10.1029/2005jd006556, 2007.

767 Jacob, D. J., Wofsy, S. C., Bakwin, P. S., Fan, S. M., Harriss, R. C., Talbot, R. W.,
768 Bradshaw, J. D., Sandholm, S. T., Singh, H. B., Browell, E. V., Gregory, G. L., Sachse, G.
769 W., Shipham, M. C., Blake, D. R., and Fitzjarrald, D. R.: Summertime photochemistry of
770 the troposphere at high northern latitudes, J. Geophys. Res, 97, 16421-16431,
771 10.1029/91jd01968, 1992.

772 Jacob, D. J.: Heterogeneous chemistry and tropospheric ozone, Atmos. Env., 34, 2131-2159,
773 2000.

774 Jacobi, H. W., Weller, R., Bluszcz, T., and Schrems, O.: Latitudinal distribution of
775 peroxyacetyl nitrate (PAN) over the Atlantic Ocean, J. Geophys. Res., 104, 26901-26912,
776 10.1029/1999jd900462, 1999.

777 Jaffe, D. A., Berntsen, T. K., and Isaksen, I. S. A.: A global three-dimensional chemical
778 transport model 2. Nitrogen oxides and nonmethane hydrocarbon results, J. Geophys. Res.,
779 102, 21281-21296, 10.1029/96jd03400, 1997.

780 Kaiser, J. W., Heil, A., Andreae, M. O., Benedetti, A., Chubarova, N., Jones, L., Morcrette,
781 J. J., Razinger, M., Schultz, M. G., Suttie, M., and van der Werf, G. R.: Biomass burning
782 emissions estimated with a global fire assimilation system based on observed fire radiative
783 power, Biogeosci., 9, 527-554, 10.5194/bg-9-527-2012, 2012.

784 Kasibhatla, P. S., Levy, H., and Moxim, W. J.: Global NO_x , HNO_3, PAN, and NO_y
785 distributions from fossil fuel combustion emissions: A model study, J. Geophys. Res, 98,
786 7165-7180, 10.1029/92jd02845, 1993.

787 Kotchenruther, R. A., Jaffe, D. A., and Jaeglé, L.: Ozone photochemistry and the role of
788 peroxyacetyl nitrate in the springtime northeastern Pacific troposphere: Results from the
789 Photochemical Ozone Budget of the Eastern North Pacific Atmosphere (PHOBEA)
790 campaign, J. Geophys. Res., 106, 28731-28742, 10.1029/2000jd000060, 2001.

791 Kuhns, H., Green, M., and Etyemezian, V.: Big Bend Regional Aerosol and Visibility
792 Observational (BRAVO) Study Emissions Inventory, Desert Research Institute, Las Vegas,
793 NV, 2003.

794 Labrador, L. J., von Kuhlmann, R., and Lawrence, M. G.: The effects of lightning-produced
795 NOx and its vertical distribution on atmospheric chemistry: sensitivity simulations with
796 MATCH-MPIC, Atmos. Chem. Phys., 5, 1815-1834, 10.5194/acp-5-1815-2005, 2005.

Lelieveld, J., Butler, T. M., Crowley, J. N., Dillon, T. J., Fischer, H., Ganzeveld, L., Harder, H., Lawrence, M. G., Martinez, M., Taraborrelli, D., and Williams, J.: Atmospheric oxidation capacity sustained by a tropical forest, Nature, 452, 737-740, http://www.nature.com/nature/journal/v452/n7188/suppinfo/nature06870_S1.html, 2008.

Leung, F.-Y. T., Logan, J. A., Park, R., Hyer, E., Kasischke, E., Streets, D., and Yurganov, L.: Impacts of enhanced biomass burning in the boreal forests in 1998 on tropospheric chemistry and the sensitivity of model results to the injection height of emissions, J. Geophys. Res., 112, D10313, 10.1029/2006jd008132, 2007.

Liang, H., Z. M. Chen, D. Huang, Y. Zhao, and Z. Y. Li: , Impacts of aerosols on the chemistry of atmospheric trace gases: a case study of peroxides and HO_2 radicals, Atmos. Chem. Phys., 13(22), 11259-11276, doi:10.5194/acp-13-11259-2013, 2013.

Liang, Q., Rodriguez, J. M., Douglass, A. R., Crawford, J. H., Olson, J. R., Apel, E., Bian, H., Blake, D. R., Brune, W., Chin, M., Colarco, P. R., da Silva, A., Diskin, G. S., Duncan, B. N., Huey, L. G., Knapp, D. J., Montzka, D. D., Nielsen, J. E., Pawson, S., Riemer, D. D., Weinheimer, A. J., and Wisthaler, A.: Reactive nitrogen, ozone and ozone production in the Arctic troposphere and the impact of stratosphere-troposphere exchange, Atmos. Chem. Phys., 11, 13181-13199, 10.5194/acp-11-13181-2011, 2011.

Liu, Z., Wang, Y., Gu, D., Zhao, C., Huey, L. G., Stickel, R., Liao, J., Shao, M., Zhu, T., Zeng, L., Liu, S.-C., Chang, C.-C., Amoroso, A., and Costabile, F.: Evidence of Reactive Aromatics As a Major Source of Peroxy Acetyl Nitrate over China, Environ. Sci. Tech., 44, 7017-7022, 10.1021/es1007966, 2010.

Lurmann, F. W., Lloyd, A. C., and Atkinson, R.: A Chemical Mechanism for Use in Long-Range Transport/Acid Deposition Computer Modeling, J. Geophys. Res., 91, 10905-10936, 10.1029/JD091iD10p10905, 1986.

Macdonald, A. M., Anlauf, K. G., Leaitch, W. R., Chan, E., and Tarasick, D. W.: Interannual variability of ozone and carbon monoxide at the Whistler high elevation site: 2002‚Äì2006, Atmos. Chem. Phys., 11, 11431-11446, 10.5194/acp-11-11431-2011, 2011.

Maloney, J. C., Fuelberg, H. E., Avery, M. A., Crawford, J. H., Blake, D. R., Heikes, B. G., Sachse, G. W., Sandholm, S. T., Singh, H., and Talbot, R. W.: Chemical characteristics of air from different source regions during the second Pacific Exploratory Mission in the Tropics (PEM-Tropics B), J. Geophys. Res., 106, 32609-32625, 10.1029/2001jd900100, 2001.

Mao, J., Jacob, D. J., Evans, M. J., Olson, J. R., Ren, X., Brune, W. H., Clair, J. M. S., Crounse, J. D., Spencer, K. M., Beaver, M. R., Wennberg, P. O., Cubison, M. J., Jimenez, J. L., Fried, A., Weibring, P., Walega, J. G., Hall, S. R., Weinheimer, A. J., Cohen, R. C., Chen, G., Crawford, J. H., McNaughton, C., Clarke, A. D., Jaegle, L., Fisher, J. A., Yantosca, R. M., Le Sager, P., and Carouge, C.: Chemistry of hydrogen oxide radicals (HOx) in the Arctic troposphere in spring, Atmos. Chem. Phys., 10, 5823-5838, 10.5194/acp-10-5823-2010, 2010.

837 Mao, J., Ren, X., Zhang, L., Van Duin, D. M., Cohen, R. C., Park, J. H., Goldstein, A. H.,
838 Paulot, F., Beaver, M. R., Crounse, J. D., Wennberg, P. O., DiGangi, J. P., Henry, S. B.,
839 Keutsch, F. N., Park, C., Schade, G. W., Wolfe, G. M., Thornton, J. A., and Brune, W. H.:
840 Insights into hydroxyl measurements and atmospheric oxidation in a California forest,
841 Atmos. Chem. Phys., 12, 8009-8020, 10.5194/acp-12-8009-2012, 2012.

842 Mao, J., Fan, S., Jacob, D. J., and Travis, K. R.: Radical loss in the atmosphere from Cu-Fe
843 redox coupling in aerosols, Atmos. Chem. Phys., 13, 509-519, 10.5194/acp-13-509-2013,
844 2013a.

845 Mao, J., Paulot, F., Jacob, D. J., Cohen, R. C., Crounse, J. D., Wennberg, P. O., Keller, C.
846 A., Hudman, R. C., Barkley, M. P., and Horowitz, L. W.: Ozone and organic ntrates over
847 the eastern United States: sensitivity to isoprene chemistry, J. Geophys. Res., submitted,
848 2013b.

849 Marais, E. A., Jacob, D. J., Kurosu, T. P., Chance, K., Murphy, J. G., Reeves, C., Mills, G.,
850 Casadio, S., Millet, D. B., Barkley, M. P., Paulot, F., and Mao, J.: Isoprene emissions in
851 Africa inferred from OMI observations of formaldehyde columns, Atmos. Chem. Phys.
852 Discuss., 12, 7475-7520, 10.5194/acpd-12-7475-2012, 2012.

853 Marecal, V., Pirre, M., Rivire, E. D., Pouvesle, N., Crowley, J. N., Freitas, S. R., and Longo,
854 K. M.: Modelling the reversible uptake of chemical species in the gas phase by ice particles
855 formed in a convective cloud, Atmos. Chem. Phys., 10, 4977-5000, 10.5194/acp-10-4977-
856 2010, 2010.

857 McFadyen, G. G., and Neil Cape, J.: Physical and chemical influences on PAN
858 concentrations at a rural site, Atmos. Env., 33, 2929-2940, http://dx.doi.org/10.1016/S1352-
859 2310(99)00095-3, 1999.

860 Millet, D. B., Guenther, A., Siegel, D. A., Nelson, N. B., Singh, H. B., de Gouw, J. A.,
861 Warneke, C., Williams, J., Eerdekens, G., Sinha, V., Karl, T., Flocke, F., Apel, E., Riemer,
862 D. D., Palmer, P. I., and Barkley, M.: Global atmospheric budget of acetaldehyde: 3-D
863 model analysis and constraints from in-situ and satellite observations, Atmos. Chem. Phys.,
864 10, 3405-3425, 10.5194/acp-10-3405-2010, 2010.

865 Mitovski, T., Folkins, I., Martin, R. V., and Cooper, M.: Testing convective transport on
866 short time scales: Comparisons with mass divergence and ozone anomaly patterns about
867 high rain events, J. Geophys. Res., 117, D02109, 10.1029/2011jd016321, 2012.

868 Moore, D. P., and Remedios, J. J.: Seasonality of Peroxyacetyl nitrate (PAN) in the upper
869 troposphere and lower stratosphere using the MIPAS-E instrument, Atmos. Chem. Phys., 10,
870 6117-6128, 10.5194/acp-10-6117-2010, 2010.

871 Moxim, W. J., Levy, H., II, and Kasibhatla, P. S.: Simulated global tropospheric PAN: Its
872 transport and impact on NOx, J. Geophys. Res., 101, 12621-12638, 10.1029/96jd00338,
873 1996.

874 Murphy, J. G., Oram, D. E., and Reeves, C. E.: Measurements of volatile organic
875 compounds over West Africa, Atmos. Chem. Phys., 10, 5281-5294, 10.5194/acp-10-5281-
876 2010, 2010.

877 Murray, L. T., Jacob, D. J., Logan, J. A., Hudman, R. C., and Koshak, W. J.: Optimized
878 regional and interannual variability of lightning in a global chemical transport model
879 constrained by LIS/OTD satellite data, J. Geophys. Res, in press, 2012.

880 Nishino, N., Arey, J., and Atkinson, R.: Formation Yields of Glyoxal and Methylglyoxal
881 from the Gas-Phase OH Radical-Initiated Reactions of Toluene, Xylenes, and
882 Trimethylbenzenes as a Function of NO_2 Concentration, J. Phys. Chem. A, 114, 10140-
883 10147, 10.1021/jp105112h, 2010.

884 Olivier, J. G. J., and Berdowski, J. J. M.: Global emissions sources and sinks, in: The
885 Climate System, edited by: Berdowski, J., Guicherit, R., and Heij, B. J., A. A. Balkema
886 Publishers/Swets & Zeitlinger Publishers, Lisse, The Netherlands, 33-78, 2001.

887 Oltmans, S. J., Lefohn, A. S., Harris, J. M., Tarasick, D. W., Thompson, A. M., Wernli, H.,
888 Johnson, B. J., Novelli, P. C., Montzka, S. A., Ray, J. D., Patrick, L. C., Sweeney, C.,
889 Jefferson, A., Dann, T., Davies, J., Shapiro, M., and Holben, B. N.: Enhanced ozone over
890 western North America from biomass burning in Eurasia during April 2008 as seen in
891 surface and profile observations, Atmos. Env., 44, 4497-4509,
892 10.1016/j.atmosenv.2010.07.004, 2010.

893 Orlando, J. J., Tyndall, G. S., and Calvert, J. G.: Thermal decomposition pathways for
894 peroxyacetyl nitrate (PAN): Implications for atmospheric methyl nitrate levels, Atmos. Env..
895 Part A. General Topics, 26, 3111-3118, http://dx.doi.org/10.1016/0960-1686(92)90468-Z,
896 1992.

897 Pandey Deolal, S., Staehelin, J., Brunner, D., Cui, J., Steinbacher, M., Zellweger, C., Henne,
898 S., and Vollmer, M. K.: Transport of PAN and NO_y from different source regions to the
899 Swiss high alpine site Jungfraujoch, Atmos. Env., 64, 103-115,
900 http://dx.doi.org/10.1016/j.atmosenv.2012.08.021, 2013.

901 Parrish, D. D., Dunlea, E. J., Atlas, E. L., Schauffler, S., Donnelly, S., Stoud, V., Goldstein,
902 A. H., Millet, D. B., McKay, M., Jaffe, D. A., Price, H. U., Hess, P. G., Flocke, F., and
903 Roberts, J. M.: Changes in the photochemical environment of the temperature North Pacific
904 troposphere in response to increased Asian emissions, J. Geophys. Res, 109,
905 doi:10.1029/2004JD004978, 2004.

906 Paulot, F., Crounse, J. D., Kjaergaard, H. G., Kroll, J. H., Seinfeld, J. H., and Wennberg, P.
907 O.: Isoprene photooxidation: new insights into the production of acids and organic nitrates,
908 Atmos. Chem. Phys., 9, 1479-1501, 10.5194/acp-9-1479-2009, 2009a.

909 Paulot, F., Crounse, J. D., Kjaergaard, H. G., Kürten, A., St. Clair, J. M., Seinfeld, J. H., and
910 Wennberg, P. O.: Unexpected Epoxide Formation in the Gas-Phase Photooxidation of
911 Isoprene, Science, 325, 730-733, 10.1126/science.1172910, 2009b.

912 Paulot, F., Henze, D. K., and Wennberg, P. O.: Impact of the isoprene photochemical
913 cascade on tropical ozone, Atmos. Chem. Phys., 12, 1307-1325, 10.5194/acp-12-1307-2012,
914 2012.

915 Peeters, J., Nguyen, T. L., and Vereecken, L.: HO_x radical regeneration in the oxidation of
916 isoprene, Phys. Chem. Chem. Phys., 11, 5935-5939, 2009.

917 Penkett, S. A., and Brice, K. A.: The spring maximum in photo-oxidants in the Northern
918 Hemisphere troposphere, Nature, 319, 655-657, 1986.

919 Pollack, I. B., Ryerson, T. B., Trainer, M., Neuman, J. A., Roberts, J. M., and Parrish, D. D.:
920 Trends in ozone, its precursors, and related secondary oxidation products in Los Angeles,
921 California: A synthesis of measurements from 1960 to 2010, J. Geophys. Res, 118, 5893-
922 5911, 10.1002/jgrd.50472, 2013.

923 Ran, L., Zhao, C., Geng, F., Tie, X., Tang, X., Peng, L., Zhou, G., Yu, Q., Xu, J., and
924 Guenther, A.: Ozone photochemical production in urban Shanghai, China: Analysis based
925 on ground level observations, J. Geophys. Res, 114, D15301, 10.1029/2008jd010752, 2009.

926 Roberts, J. M., and Bertman, S. B.: The thermal decomposition of peroxyacetic nitric
927 anhydride (PAN) and peroxymethacrylic nitric anhydride (MPAN), Int. J. Chem. Kin., 24,
928 297-307, 10.1002/kin.550240307, 1992.

929 Roberts, J. M., Tanner, R. L., Newman, L., Bowersox, V. C., Bottenheim, J. W., Anlauf, K.
930 G., Brice, K. A., Parrish, D. D., Fehsenfeld, F. C., Buhr, M. P., Meagher, J. F., and Bailey, E.
931 M.: Relationships between PAN and ozone at sites in eastern North America, J. Geophys.
932 Res, 100, 22821-22830, 10.1029/95jd01221, 1995.

933 Roberts, J. M., Parrish, D. D., Norton, R. B., Bertman, S. B., Holloway, J. S., Trainer, M.,
934 Fehsenfeld, F. C., Carroll, M. A., Albercook, G. M., Wang, T., and Forbes, G.: Episodic
935 removal of NO_y species from the marine boundary layer over the North Atlantic, J. Geophys.
936 Res., 101, 28947-28960, 10.1029/96jd02632, 1996.

937 Roberts, J. M., Williams, J., Baumann, K., Buhr, M. P., Goldan, P. D., Holloway, J., Hübler,
938 G., Kuster, W. C., McKeen, S. A., Ryerson, T. B., Trainer, M., Williams, E. J., Fehsenfeld,
939 F. C., Bertman, S. B., Nouaime, G., Seaver, C., Grodzinsky, G., Rodgers, M., and Young, V.
940 L.: Measurements of PAN, PPN, and MPAN made during the 1994 and 1995 Nashville
941 Intensives of the Southern Oxidant Study: Implications for regional ozone production from
942 biogenic hydrocarbons, J. Geophys. Res, 103, 22473-22490, 10.1029/98jd01637, 1998.

943 Roberts, J. M., Flocke, F., Stroud, C. A., Hereid, D., Williams, E., Fehsenfeld, F., Brune, W.,
944 Martinez, M., and Harder, H.: Ground-based measurements of peroxycarboxylic nitric
945 anhydrides (PANs) during the 1999 Southern Oxidants Study Nashville Intensive, J.
946 Geophys. Res, 107, ACH 1-1-ACH 1-10, 10.1029/2001jd000947, 2002.

947 Roberts, J. M., Flocke, F., Chen, G., de Gouw, J., Holloway, J. S., H¸bler, G., Neuman, J. A.,
948 Nicks, D. K., Jr., Nowak, J. B., Parrish, D. D., Ryerson, T. B., Sueper, D. T., Warneke, C.,
949 and Fehsenfeld, F. C.: Measurement of peroxycarboxylic nitric anhydrides (PANs) during

the ITCT 2K2 aircraft intensive experiment, J. Geophys. Res., 109, D23S21, 10.1029/2004jd004960, 2004.

Roberts, J. M.: Measurement of the Henry's law coefficient and first order loss rate of PAN in n-octanol, Geophys. Res. Lett., 32, L08803, 10.1029/2004gl022327, 2005.

Roberts, J. M., Marchewka, M., Bertman, S. B., Goldan, P., Kuster, W., de Gouw, J., Warneke, C., Williams, E., Lerner, B., Murphy, P., Apel, E., and Fehsenfeld, F. C.: Analysis of the isoprene chemistry observed during the New England Air Quality Study (NEAQS) 2002 intensive experiment, J. Geophys. Res., 111, D23S12, 10.1029/2006jd007570, 2006.

Roberts, J. M.: PAN and Related Compounds, in: Volatile Organic Compounds in the Atmosphere, Blackwell Publishing Ltd, 221-268, 2007.

Roiger, A., Aufmhoff, H., Stock, P., Arnold, F., and Schlager, H.: An aircraft-borne chemical ionization - ion trap mass spectrometer (CI-ITMS) for fast PAN and PPN measurements, Atmos. Meas. Tech., 4, 173-188, 10.5194/amt-4-173-2011, 2011.

Sander, S. P., J. Abbatt, J. R. Barker, J. B. Burkholder, R. R. Friedl, D. M. Golden, R. E. Huie, C. E. Kolb, M. J. Kurylo, G. K. Moortgat, V. L. Orkin and P. H. Wine "Chemical Kinetics and Photochemical Data for Use in Atmospheric Studies, Evaluation No. 17," JPL Publication 10-6, Jet Propulsion Laboratory, Pasedena, 2011 http://jpldataeval.jpl.nasa.gov.

Saunders, S. M., Jenkin, M. E., Derwent, R. G., and Pilling, M. J.: Protocol for the development of the Master Chemical Mechanism, MCM v3 (Part A): tropospheric degradation of non-aromatic volatile organic compounds, Atmos. Chem. Phys., 3, 161-180, 10.5194/acp-3-161-2003, 2003.

Sauvage, B., Martin, R. V., van Donkelaar, A., Liu, X., Chance, K., L., J., Palmer, P. I., Wu, S., and Fu, T. M.: Remote sensed and in situ constraints on processes affecting tropical tropospheric ozone, Atmos. Chem. Phys., 7, 815-838, 10.5194/acp-7-815-2007, 2007.

Shepson, P. B., Bottenheim, J. W., Hastie, D. R., and Venkatram, A.: Determination of the relative ozone and PAN deposition velocities at night, Geophys. Res. Lett., 19, 1121-1124, 10.1029/92gl01118, 1992.

Sillman, S., and Samson, P. J.: Impact of temperature on oxidant photochemistry in urban, polluted rural and remote environments, J. Geophys. Res, 100, 11497-11508, 10.1029/94jd02146, 1995.

Singh, H. B., and Hanst, P. L.: Peroxyacetyl nitrate (PAN) in the unpolluted atmosphere: An important reservoir for nitrogen oxides, Geophys. Res. Lett., 8, 941-944, 10.1029/GL008i008p00941, 1981.

Singh, H. B.: Reactive nitrogen in the troposphere: chemistry and transport of NOx and PAN, Environ. Sci. Tech., 21, 1987.

Emily Fischer 1/12/14 1:07 PM
Formatted: Font:Italic

Emily Fischer 1/12/14 1:07 PM
Deleted: Sehested, J., Christensen, L. K., Møgelberg, T., Nielsen, O. J., Wallington, T. J., Orlando, J., and Tyndall, G. S.: Absolute and Relative Rate Constants for the Reactions CH3C(O)O2 + NO and CH3C(O)O2 + NO2 and Thermal Stability of CH3C(O)O2NO2, J. Phys. Chem. A, 102, 1779-1789, 10.1021/jp972881a, 1998.

994 Singh, H. B., Condon, E., Vedder, J., O'Hara, D., Ridley, B. A., Gandrud, B. W., Shetter, J.
995 D., Salas, L. J., Huebert, B., H¸bler, G., Carroll, M. A., Albritton, D. L., Davis, D. D.,
996 Bradshaw, J. D., Sandholm, S. T., Rodgers, M. O., Beck, S. M., Gregory, G. L., and LeBel,
997 P. J.: Peroxyacetyl Nitrate Measurements During CITE 2: Atmospheric Distribution and
998 Precursor Relationships, J. Geophys. Res., 95, 10163-10178, 10.1029/JD095iD07p10163,
999 1990a.

1000 Singh, H. B., Herlth, D., O'Hara, D., Salas, L., Torres, A. L., Gregory, G. L., Sachse, G. W.,
1001 and Kasting, J. F.: Atmospheric Peroxyacetyl Nitrate Measurements Over the Brazilian
1002 Amazon Basin During the Wet Season: Relationships With Nitrogen Oxides and Ozone, J.
1003 Geophys. Res., 95, 16945-16954, 10.1029/JD095iD10p16945, 1990b.

1004 Singh, H. B., Herlth, D., O'Hara, D., Zahnle, K., Bradshaw, J. D., Sandholm, S. T., Talbot,
1005 R., Crutzen, P. J., and Kanakidou, M.: Relationship of Peroxyacetyl Nitrate to Active and
1006 Total Odd Nitrogen at Northern High Latitudes: Influence of Reservoir Species on NO_x and
1007 O_3, J. Geophys. Res., 97, 16523-16530, 10.1029/91jd00890, 1992.

1008 Singh, H. B., Herlth, D., O'Hara, D., Zahnle, K., Bradshaw, J. D., Sandholm, S. T., Talbot,
1009 R., Gregory, G. L., Sachse, G. W., Blake, D. R., and Wofsy, S. C.: Summertime distribution
1010 of PAN and other reactive nitrogen species in the northern high-latitude atmosphere of
1011 eastern Canada, J. Geophys. Res., 99, 1821-1835, 10.1029/93jd00946, 1994.

1012 Singh, H. B., Kanakidou, M., Crutzen, P. J., and Jacob, D. J.: High concentrations and
1013 photochemical fate of oxygenated hydrocarbons in the global troposphere, Nature, 378, 50-
1014 54, 1995.

1015 Singh, H. B., Herlth, D., Kolyer, R., Chatfield, R., Viezee, W., Salas, L. J., Chen, Y.,
1016 Bradshaw, J. D., Sandholm, S. T., Talbot, R., Gregory, G. L., Anderson, B., Sachse, G. W.,
1017 Browell, E., Bachmeier, A. S., Blake, D. R., Heikes, B., Jacob, D., and Fuelberg, H. E.:
1018 Impact of biomass burning emissions on the composition of the South Atlantic troposphere:
1019 Reactive nitrogen and ozone, J. Geophys. Res., 101, 24203-24219, 10.1029/96jd01018,
1020 1996a.

1021 Singh, H. B., Herlth, D., Kolyer, R., Salas, L., Bradshaw, J. D., Sandholm, S. T., Davis, D.
1022 D., Crawford, J., Kondo, Y., Koike, M., Talbot, R., Gregory, G. L., Sachse, G. W., Browell,
1023 E., Blake, D. R., Rowland, F. S., Newell, R., Merrill, J., Heikes, B., Liu, S. C., Crutzen, P. J.,
1024 and Kanakidou, M.: Reactive nitrogen and ozone over the western Pacific: Distribution,
1025 partitioning, and sources, J. Geophys. Res., 101, 1793-1808, 10.1029/95jd01029, 1996b.

1026 Singh, H. B., Viezee, W., Chen, Y., Thakur, A. N., Kondo, Y., Talbot, R. W., Gregory, G.
1027 L., Sachse, G. W., Blake, D. R., Bradshaw, J. D., Wang, Y., and Jacob, D. J.: Latitudinal
1028 distribution of reactive nitrogen in the free troposphere over the Pacific Ocean in late
1029 winter/early spring, J. Geophys. Res., 103, 28237-28246, 10.1029/98jd01891, 1998.

1030 Singh, H. B., Brune, W. H., Crawford, J. H., Jacob, D. J., and Russell, P. B.: Overview of
1031 the summer 2004 Intercontinental Chemical Transport Experiment-North America (INTEX-
1032 A), J. Geophys. Res., 111, D24S01, 10.1029/2006jd007905, 2006.

Singh, H. B., Salas, L., Herlth, D., Kolyer, R., Czech, E., Avery, M., Crawford, J. H., Pierce, R. B., Sachse, G. W., Blake, D. R., Cohen, R. C., Bertram, T. H., Perring, A., Wooldridge, P. J., Dibb, J., Huey, G., Hudman, R. C., Turquety, S., Emmons, L. K., Flocke, F., Tang, Y., Carmichael, G. R., and Horowitz, L. W.: Reactive nitrogen distribution and partitioning in the North American troposphere and lowermost stratosphere, J. Geophys. Res., 112, D12S04, 10.1029/2006jd007664, 2007.

Singh, H. B., Brune, W. H., Crawford, J. H., Flocke, F., and Jacob, D. J.: Chemistry and transport of pollution over the Gulf of Mexico and the Pacific: spring 2006 INTEX-B campaign overview and first results, Atmos. Chem. Phys., 9, 2301-2318, 10.5194/acp-9-2301-2009, 2009.

Slusher, D. L., Huey, L. G., Tanner, D. J., Flocke, F. M., and Roberts, J. M.: A thermal dissociation chemical ionization mass spectrometry (TD-CIMS) technique for the simultaneous measurement of peroxyacyl nitrates and dinitrogen pentoxide, J. Geophys. Res., 109, D19315, 10.1029/2004jd004670, 2004.

Smyth, S. B., Sandholm, S. T., Bradshaw, J. D., Talbot, R. W., Blake, D. R., Blake, N. J., Rowland, F. S., Singh, H. B., Gregory, G. L., Anderson, B. E., Sachse, G. W., Collins, J. E., and Bachmeier, A. S.: Factors influencing the upper free tropospheric distribution of reactive nitrogen over the South Atlantic during the TRACE A experiment, J. Geophys. Res., 101, 24165-24186, 10.1029/96jd00224, 1996.

Stewart, D. J., Taylor, C. M., Reeves, C. E., and McQuaid, J. B.: Biogenic nitrogen oxide emissions from soils: impact on NO_x and ozone over west Africa during AMMA (African Monsoon Multidisciplinary Analysis): observational study, Atmos. Chem. Phys., 8, 2285-2297, 10.5194/acp-8-2285-2008, 2008.

Stone, D., Evans, M. J., Walker, H. M., Ingham, T., Vaughan, S., Ouyang, B., Kennedy, O. J., McLeod, M. W., Jones, R. L., Hopkins, J., Punjabi, S., Lidster, R., Hamilton, J. F., Lee, J. D., Lewis, A. C., Carpenter, L. J., Forster, G., Oram, D. E., Reeves, C. E., Bauguitte, S., Morgan, W., Coe, H., Aruffo, E., Dari-Salisburgo, C., Giammaria, F., Di Carlo, P., and Heard, D. E.: Radical chemistry at night: comparisons between observed and modelled HO_x, NO_3 and N_2O_5 during the RONOCO project, Atmos. Chem. Phys. Discuss., 13, 9519-9566, doi:10.5194/acpd-13-9519-2013, 2013.

Stroud, C., Madronich, S., Atlas, E., Cantrell, C., Fried, A., Wert, B., Ridley, B., Eisele, F., Mauldin, L., Shetter, R., Lefer, B., Flocke, F., Weinheimer, A., Coffey, M., Heikes, B., Talbot, R., and Blake, D.: Photochemistry in the Arctic Free Troposphere: Ozone Budget and Its Dependence on Nitrogen Oxides and the Production Rate of Free Radicals, J.of Atmos. Chem., 47, 107-138, 10.1023/B:JOCH.0000021026.71906.e1, 2004.

Sudo, K., Takahashi, M., and Akimoto, H.: CHASER: A global chemical model of the troposphere 2. Model results and evaluation, J. Geophys. Res, 107, 4586, 10.1029/2001jd001114, 2002.

Talbot, R., Dibb, J., Scheuer, E., Seid, G., Russo, R., Sandholm, S., Tan, D., Singh, H., Blake, D., Blake, N., Atlas, E., Sachse, G., Jordan, C., and Avery, M.: Reactive nitrogen in

Emily Fischer 1/12/14 11:33 AM

Deleted: Stone, D., Evans, M. J., Bunyan, H., Ingham, T., Vaughan, S., Ouyang, B., Kennedy, O. J., McLeod, M. W., Jones, R. L., Hopkins, J., Punjabi, S., Lidster, R., Hamilton, J. F., Lee, J. D., Lewis, A. C., Carpenter, L. J., Bauguitte, S., Morgan, W., Coe, H., Aruffo, E., Dari-Salisburgo, C., Giammaria, F., Carlo, P. D., and Heard, D. E.: Radical Chemistry at Night: Comparisons between observed and modelled HO_x, NO_3 and N_2O_5 during the RONOCO project, Atmos. Chem.and Phys., in preparation, 2013.

1085 Asian continental outflow over the western Pacific: Results from the NASA Transport and
1086 Chemical Evolution over the Pacific (TRACE-P) airborne mission, J. Geophys. Res., 108,
1087 8803, 10.1029/2002jd003129, 2003.

1088 Talbot, R. W., Dibb, J. E., Scheuer, E. M., Kondo, Y., Koike, M., Singh, H. B., Salas, L. B.,
1089 Fukui, Y., Ballenthin, J. O., Meads, R. F., Miller, T. M., Hunton, D. E., Viggiano, A. A.,
1090 Blake, D. R., Blake, N. J., Atlas, E., Flocke, F., Jacob, D. J., and Jaegle, L.: Reactive
1091 nitrogen budget during the NASA SONEX Mission, Geophys. Res. Lett., 26, 3057-3060,
1092 10.1029/1999gl900589, 1999.

1093 Talbot, R. W., Dibb, J. E., Scheuer, E. M., Bradshaw, J. D., Sandholm, S. T., Singh, H. B.,
1094 Blake, D. R., Blake, N. J., Atlas, E., and Flocke, F.: Tropospheric reactive odd nitrogen over
1095 the South Pacific in austral springtime, J. Geophys. Res., 105, 6681-6694,
1096 10.1029/1999jd901114, 2000.

1097 Talukdar, R. K., Burkholder, J. B., Schmoltner, A.-M., Roberts, J. M., Wilson, R. R., and
1098 Ravishankara, A. R.: Investigation of the loss processes for peroxyacetyl nitrate in the
1099 atmosphere: UV photolysis and reaction with OH, J. Geophys. Res., 100, 14163-14173,
1100 10.1029/95jd00545, 1995.

1101 Tanimoto, H., Wild, O., Kato, S., Furutani, H., Makide, Y., Komazaki, Y., Hashimoto, S.,
1102 Tanaka, S., and Akimoto, H.: Seasonal cycles of ozone and oxidized nitrogen species in
1103 northeast Asia 2. A model analysis of the roles of chemistry and transport, J. Geophys. Res.,
1104 107, 4706, 10.1029/2001jd001497, 2002.

1105 Tereszchuk, K. A., Moore, D. P., Harrison, J. J., Boone, C. D., Park, M., Remedios, J. J.,
1106 Randel, W. J., and Bernath, P. F.: Observations of peroxyacetyl nitrate (PAN) in the upper
1107 troposphere by the Atmospheric Chemistry Experiment-Fourier Transform Spectrometer
1108 (ACE-FTS), Atmos. Chem. Phys., 13, 5601-5613, 10.5194/acp-13-5601-2013, 2013.

1109 Thakur, A. N., Singh, H. B., Mariani, P., Chen, Y., Wang, Y., Jacob, D. J., Brasseur, G.,
1110 Müller, J. F., and Lawrence, M.: Distribution of reactive nitrogen species in the remote free
1111 troposphere: data and model comparisons, Atmos. Env., 33, 1403-1422, 10.1016/s1352-
1112 2310(98)00281-7, 1999.

1113 Thornton, J. A., Jaegle, L., and McNeill, V. F.: Assessing known pathways for HO_2 loss in
1114 aqueous atmospheric aerosols: Regional and global impacts on tropospheric oxidants,
1115 Journal of Geophysical Research, 113, doi:10.1029/2007JD009236, 2008.

1116 Tie, X., Zhang, R., Brasseur, G., Emmons, L., and Lei, W.: Effects of lightning on reactive
1117 nitrogen and nitrogen reservoir species in the troposphere, J. Geophys. Res., 106, 3167-3178,
1118 10.1029/2000jd900565, 2001.

1119 Turquety, S., Logan, J. A., Jacob, D. J., Hudman, R. C., Leung, F. Y., Heald, C. L.,
1120 Yantosca, R. M., Wu, S., Emmons, L. K., Edwards, D. P., and Sachse, G. W.: Inventory of
1121 boreal fire emissions for North America in 2004: Importance of peat burning and
1122 pyroconvective injection, J. Geophys. Res., 112, D12S03, 10.1029/2006jd007281, 2007.

1123 Tyndall, G. S., Cox, R. A., Granier, C., Lesclaux, R., Moortgat, G. K., Pilling, M. J.,
1124 Ravishankara, A. R., and Wallington, T. J.: Atmospheric chemistry of small organic peroxy
1125 radicals, J. Geophys. Res, 106, 12157-12182, 10.1029/2000jd900746, 2001.

1126 Val Martin, M., Honrath, R. E., Owen, R. C., and Li, Q. B.: Seasonal variation of nitrogen
1127 oxides in the central North Atlantic lower free troposphere, J. Geophys. Res, 113, D17307,
1128 10.1029/2007jd009688, 2008.

1129 Val Martin, M., Logan, J. A., Kahn, R. A., Leung, F. Y., Nelson, D. L., and Diner, D. J.:
1130 Smoke injection heights from fires in North America: analysis of 5 years of satellite
1131 observations, Atmos. Chem. Phys., 10, 1491-1510, 10.5194/acp-10-1491-2010, 2010.

1132 van der A, R. J., Eskes, H. J., Boersma, K. F., van Noije, T. P. C., Van Roozendael, M., De
1133 Smedt, I., Peters, D. H. M. U., and Meijer, E. W.: Trends, seasonal variability and dominant
1134 NO_x source derived from a ten year record of NO_2 measured from space, J. Geophys. Res.,
1135 113, D04302, 10.1029/2007jd009021, 2008.

1136 van der Werf, G. R., Randerson, J. T., Giglio, L., Collatz, G. J., Mu, M., Kasibhatla, P. S.,
1137 Morton, D. C., DeFries, R. S., Jin, Y., and van Leeuwen, T. T.: Global fire emissions and
1138 the contribution of deforestation, savanna, forest, agricultural, and peat fires (1997-2009),
1139 Atmos. Chem. Phys., 10, 11707-11735, 10.5194/acp-10-11707-2010, 2010.

1140 van Donkelaar, A., Martin, R. V., Leaitch, W. R., Macdonald, A. M., Walker, T. W., Streets,
1141 D. G., Zhang, Q., Dunlea, E. J., Jimenez, J. L., Dibb, J. E., Huey, L. G., Weber, R., and
1142 Andreae, M. O.: Analysis of aircraft and satellite measurements from the Intercontinental
1143 Chemical Transport Experiment (INTEX-B) to quantify long-range transport of East Asian
1144 sulfur to Canada, Atmos. Chem. Phys., 8, 2999-3014, 10.5194/acp-8-2999-2008, 2008.

1145 van het Bolscher, M., Pereira, J., Spessa, A., Dalsoren, S., van Nojie, T., and Szopa, S.:
1146 REanalysis of the TROpospheric chemical composition over the past 40 years: A long-term
1147 global modeling study of tropospheric chemistry, Max Plank Inst. for Meteorology,
1148 Hamburg, Germany, 77, 2008.

1149 Vestreng, V., and Klein, H.: Emission data reported to UNECE/EMEP: Quality assurance
1150 and trend analysis & presentation of WebDab, Norwegian Meteorological Institute, Oslo,
1151 Norway, 2002.

1152 Villalta, P. W., Lovejoy, E. R., and Hanson, D. R.: Reaction probability of peroxyacetyl
1153 radical on aqueous surfaces, Geophys. Res. Lett., 23, 1765-1768, 10.1029/96gl01286, 1996.

1154 Vivchar, A.: Wildfires in Russia in 2000 - 2008: estimates of burnt areas using the satellite
1155 MODIS MCD45 data, Remote Sensing Letters, 2, 81-90, 10.1080/01431161.2010.499138,
1156 2010.

1157 von Kuhlmann, R., Lawrence, M. G., Crutzen, P. J., and Rasch, P. J.: A model for studies of
1158 tropospheric ozone and nonmethane hydrocarbons: Model evaluation of ozone-related
1159 species, J. Geophys. Res, 108, 4729, 10.1029/2002jd003348, 2003.

von Kuhlmann, R., Lawrence, M. G., Poschl, U., and Crutzen, P. J.: Sensitivities in global scale modeling of isoprene, Atmos. Chem. Phys., 4, 1-17, 10.5194/acp-4-1-2004, 2004.

Walker, T. W., Jones, D. B. A., Parrington, M., Henze, D. K., Murray, L. T., Bottenheim, J. W., Anlauf, K., Worden, J. R., Bowman, K. W., Shim, C., Singh, K., Kopacz, M., Tarasick, D. W., Davies, J., von der Gathen, P., Thompson, A. M., and Carouge, C. C.: Impacts of midlatitude precursor emissions and local photochemistry on ozone abundances in the Arctic, J. Geophys. Res, 117, n/a-n/a, 10.1029/2011jd016370, 2012.

Wallington, T. J., Andino, J. M., Ball, J. C., and Japar, S. M.: Fourier transform infrared studies of the reaction of Cl atoms with PAN, PPN, CH_3OOH, HCOOH, CH_3COCH_3 and $CH_3COC_2H_5$ at 295±2 K, J. Atmos. Chem., 10, 301-313, 10.1007/bf00053865, 1990.

Wang, S., Wu, D., Wang, X.-M., Fung, J. C.-H., and Yu, J. Z.: Relative contributions of secondary organic aerosol formation from toluene, xylenes, isoprene, and monoterpenes in Hong Kong and Guangzhou in the Pearl River Delta, China: an emission-based box modeling study, J. Geophys. Res, 118, 507-519, 10.1029/2012jd017985, 2013.

Wang, X.-m., Sheng, G.-y., Fu, J.-m., Chan, C.-y., Lee, S.-C., Chan, L. Y., and Wang, Z.-s.: Urban roadside aromatic hydrocarbons in three cities of the Pearl River Delta, People's Republic of China, Atmos. Env., 36, 5141-5148, http://dx.doi.org/10.1016/S1352-2310(02)00640-4, 2002.

Wang, Y. X., M. B. McElroy, D. J. Jacob, and R. M. Yantosca, A nested grid formulation for chemical transport over Asia: Applications to CO, Journal of Geophysical Research: Atmospheres, 109(D22), D22307, 10.1029/2004JD005237, 2004.

Wang, Y., Jacob, D. J., and Logan, J. A.: Global simulation of tropospheric O3-NOx - hydrocarbon chemistry: 3. Origin of tropospheric ozone and effects of nonmethane hydrocarbons, J. Geophys. Res, 103, 10757-10767, 10.1029/98jd00156, 1998a.

Wang, Y., Logan, J. A., and Jacob, D. J.: Global simulation of tropospheric O3-NOx - hydrocarbon chemistry 2. Model evaluation and global ozone budget, J. Geophys. Res., 103, 10727-10755, 10.1029/98jd00157, 1998b.

Wang, Y., Ridley, B., Fried, A., Cantrell, C., Davis, D., Chen, G., Snow, J., Heikes, B., Talbot, R., Dibb, J., Flocke, F., Weinheimer, A., Blake, N., Blake, D., Shetter, R., Lefer, B., Atlas, E., Coffey, M., Walega, J., and Wert, B.: Springtime photochemistry at northern mid and high latitudes, J. Geophys. Res., 108, 8358, 10.1029/2002jd002227, 2003.

Warneke, C., Holzinger, R., Hansel, A., Jordan, A., Lindinger, W., P√∂schl, U., Williams, J., Hoor, P., Fischer, H., Crutzen, P. J., Scheeren, H. A., and Lelieveld, J.: Isoprene and Its Oxidation Products Methyl Vinyl Ketone, Methacrolein, and Isoprene Related Peroxides Measured Online over the Tropical Rain Forest of Surinam in March 1998, Journal of Atmospheric Chemistry, 38, 167-185, 10.1023/a:1006326802432, 2001.

Warneke, C., Bahreini, R., Brioude, J., Brock, C. A., de Gouw, J. A., Fahey, D. W., Froyd, K. D., Holloway, J. S., Middlebrook, A., Miller, L., Montzka, S., Murphy, D. M., Peischl, J.,

Emily Fischer 1/12/14 11:05 AM
Formatted: Font:Italic

Emily Fischer 1/12/14 11:05 AM
Formatted: Font:Not Italic

1198 Ryerson, T. B., Schwarz, J. P., Spackman, J. R., and Veres, P.: Biomass burning in Siberia
1199 and Kazakhstan as an important source for haze over the Alaskan Arctic in April 2008,
1200 Geophys. Res. Lett., 36, L02813, 10.1029/2008gl036194, 2009.

1201 Warneke, C., Froyd, K. D., Brioude, J., Bahreini, R., Brock, C. A., Cozic, J., de Gouw, J. A.,
1202 Fahey, D. W., Ferrare, R., Holloway, J. S., Middlebrook, A. M., Miller, L., Montzka, S.,
1203 Schwarz, J. P., Sodemann, H., Spackman, J. R., and Stohl, A.: An important contribution to
1204 springtime Arctic aerosol from biomass burning in Russia, Geophys. Res. Lett., 37, L01801,
1205 10.1029/2009gl041816, 2010.

1206 Warneke, C., Roberts, J. M., Veres, P., Gilman, J., Kuster, W. C., Burling, I., Yokelson, R.,
1207 and de Gouw, J. A.: VOC identification and inter-comparison from laboratory biomass
1208 burning using PTR-MS and PIT-MS, International Journal of Mass Spectrometry, 303, 6-14,
1209 10.1016/j.ijms.2010.12.002, 2011.

1210 Wesely, M. L.: Parameterization of surface resistances to gaseous dry deposition in
1211 regional-scale numerical models, Atmos. Env. (1967), 23, 1293-1304,
1212 http://dx.doi.org/10.1016/0004-6981(89)90153-4, 1989.

1213 Whalley, L. K., Lewis, A. C., McQuaid, J. B., Purvis, R. M., Lee, J. D., Stemmler, K.,
1214 Zellweger, C., and Ridgeon, P.: Two high-speed, portable GC systems designed for the
1215 measurement of non-methane hydrocarbons and PAN: Results from the Jungfraujoch High
1216 Altitude Observatory, J. Environ. Mon., 6, 234-241, 2004.

1217 Wiedinmyer, C., Akagi, S. K., Yokelson, R. J., Emmons, L. K., Al-Saadi, J. A., Orlando, J.
1218 J., and Soja, A. J.: The Fire INventory from NCAR (FINN): a high resolution global model
1219 to estimate the emissions from open burning, Geosci. Model Dev., 4, 625-641,
1220 10.5194/gmd-4-625-2011, 2011.

1221 Wiegele, A., Glatthor, N., Höpfner, M., Grabowski, U., Kellmann, S., Linden, A., Stiller, G.,
1222 and von Clarmann, T.: Global distributions of C_2H_6, C_2H_2, HCN, and PAN retrieved from
1223 MIPAS reduced spectral resolution measurements, Atmos. Meas. Tech., 5, 723-734,
1224 10.5194/amt-5-723-2012, 2012.

1225 Williams, J. E., van Velthoven, P. F. J., and Brenninkmeijer, C. A. M.: Quantifying the
1226 uncertainty in simulating global tropospheric composition due to the variability in global
1227 emission estimates of Biogenic Volatile Organic Compounds, Atmos. Chem. Phys., 13,
1228 2857-2891, 10.5194/acp-13-2857-2013, 2013.

1229 Wolfe, G. M., Thornton, J. A., McNeill, V. F., Jaffe, D. A., Reidmiller, D., Chand, D.,
1230 Smith, J., Swartzendruber, P., Flocke, F., and Zheng, W.: Influence of trans-Pacific
1231 pollution transport on acyl peroxy nitrate abundances and speciation at Mount Bachelor
1232 Observatory during INTEX-B, Atmos. Chem. Phys., 7, 5309-5325, 10.5194/acp-7-5309-
1233 2007, 2007.

1234 Worthy, D. E. J., Trivett, N. B. A., Hopper, J. F., and Bottenheim, J. W.: Analysis of long-
1235 range transport events at Alert, Northwest Territories, during the Polar Sunrise Experiment,
1236 J. Geophys. Res, 99, 25,329-325,344, 1994.

Xiao, Y., Logan, J. A., Jacob, D. J., Hudman, R. C., Yantosca, R., and Blake, D. R.: Global budget of ethane and regional constraints on U.S. sources, J. Geophys. Res., 113, D21306, 10.1029/2007jd009415, 2008.

Xue, L. K., Wang, T., Zhang, J. M., Zhang, X. C., Deliger, Poon, C. N., Ding, A. J., Zhou, X. H., Wu, W. S., Tang, J., Zhang, Q. Z., and Wang, W. X.: Source of surface ozone and reactive nitrogen speciation at Mount Waliguan in western China: New insights from the 2006 summer study, J. Geophys. Res., 116, D07306, 10.1029/2010jd014735, 2011.

Yienger, J. J., and Levy, H., II: Empirical model of global soil-biogenic NO_x emissions, J. Geophys. Res., 100, 11447-11464, 10.1029/95jd00370, 1995.

Zanis, P., Monks, P. S., Green, T. J., Schuepbach, E., Carpenter, L. J., Mills, G. P., Rickard, A. R., Brough, N., and Penkett, S. A.: Seasonal variation of peroxy radicals in the lower free troposphere based on observations from the FREE Tropospheric EXperiments in the Swiss Alps, Geophys. Res. Lett., 30, 1497, 10.1029/2003gl017122, 2003.

Zanis, P., Ganser, A., Zellweger, C., Henne, S., Steinbacher, M., and Staehelin, J.: Seasonal variability of measured ozone production efficiencies in the lower free troposphere of Central Europe, Atmos. Chem. Phys., 7, 223-236, 10.5194/acp-7-223-2007, 2007.

Zellweger, C., Ammann, M., Buchmann, B., Hofer, P., Lugauer, M., Rüttimann, R., Streit, N., Weingartner, E., and Baltensperger, U.: Summertime NO_y speciation at the Jungfraujoch, 3580 m above sea level, Switzerland, J. Geophys. Res., 105, 6655-6667, 10.1029/1999jd901126, 2000.

Zhang, J., Wang, T., Chameides, W. L., Cardelino, C., Kwok, J., Blake, D. R., Ding, A., and So, K. L.: Ozone production and hydrocarbon reactivity in Hong Kong, Southern China, Atmos. Chem. Phys., 7, 557-573, 10.5194/acp-7-557-2007, 2007a.

Zhang, L., Jacob, D. J., Boersma, K. F., Jaffe, D. A., Olson, J. R., Bowman, K. W., Worden, J. R., Thompson, A. M., Avery, M. A., Cohen, R. C., Dibb, J. E., Flock, F. M., Fuelberg, H. E., Huey, L. G., McMillan, W. W., Singh, H. B., and Weinheimer, A. J.: Transpacific transport of ozone pollution and the effect of recent Asian emission increases on air quality in North America: an integrated analysis using satellite, aircraft, ozonesonde, and surface observations, Atmos. Chem. Phys., 8, 6117-6136, 10.5194/acp-8-6117-2008, 2008.

Zhang, Q., Streets, D. G., He, K., Wang, Y., Richter, A., Burrows, J. P., Uno, I., Jang, C. J., Chen, D., Yao, Z., and Lei, Y.: NO_x emission trends for China, 1995-2004: The view from the ground and the view from space, J. Geophys. Res., 112, D22306, 10.1029/2007jd008684, 2007b.

Zhang, Q., Streets, D. G., Carmichael, G. R., He, K. B., Huo, H., Kannari, A., Klimont, Z., Park, I. S., Reddy, S., Fu, J. S., Chen, D., Duan, L., Lei, Y., Wang, L. T., and Yao, Z. L.: Asian emissions in 2006 for the NASA INTEX-B mission, Atmos. Chem. Phys., 9, 5131-5153, 10.5194/acp-9-5131-2009, 2009.

Zheng, W., Flocke, F. M., Tyndall, G. S., Swanson, A., Orlando, J. J., Roberts, J. M., Huey, L. G., and Tanner, D. J.: Characterization of a thermal decomposition chemical ionization mass spectrometer for the measurement of peroxy acyl nitrates (PANs) in the atmosphere, Atmos. Chem. Phys., 11, 6529-6547, 10.5194/acp-11-6529-2011, 2011.

Tables

Table 1: Global contributions of primary NMVOCs to PAN formation[a]

Primary NMVOC	Lifetime (days)[b]	Sources, Tg C a^{-1}			Molar Yields of Immediate PAN Precursors			PAN Contribution (%)[e]
		Fuel and Industry[c]	Open Fires	Biogenic	Acetaldehyde[d]	Acetone	Methyl-glyoxal	
Isoprene	0.10	-	-	427	0.019	-	0.32	37[f]
Terpenes	0.46[g]	-	1.3	65[g]	0.025[h]	0.017[h]	0.050[h]	9
>C_3 alkanes[i]	5	24	0.67	-	1.07	0.30	-	9
Acetone	14	0.45	1.7	69[j]	-	1	0.14[k]	9
Acetaldehyde	0.8	1.1	1.6	44[j]	1	-	-	8
Ethane	60	8.5	1.9	-	0.78	-	-	6
Propane	14	17	0.77	-	0.30	0.75	-	5
>C_2 alkenes[l]	0.38	3.9	2.7	12	0.85	-	-	4
Ethanol	2.8	1.0	0.04	12	0.95	-	-	4
Methyl-glyoxal	0.067	-	2.6	-	0.35[m]	-	1	< 1
Xylenes[n]	0.58	11	0.73	-	-	-	0.21	< 1
Toluene[o]	2.2	14	0.26	-	-	-	0.46	< 1
Hydroxy-acetone	2.1	-	0.65	-	-	-	0.82[p]	< 1
Methyl ethyl ketone	4.3	0.34	0.99	-	0.002	-	-	< 1

[a] Global primary emitted NMVOC sources of PAN and their estimated yields for the three most important immediate carbonyl PAN precursors: acetaldehyde, acetone, and methylglyoxal. Details of sources can be found in Section 2.2.
[b] Global annual mean tropospheric lifetime. Lifetimes were calculated from global annual average burdens and loss rates.
[c] Includes biofuel use
[d] Assumes 1 ppbv NO_x from Millet et al. (2010) unless otherwise noted
[e] The contribution to the global annual PAN burden from individual NMVOCs is calculated Contribution to global annual mean PAN calculated by simulations with corresponding emissions turned off. To avoid large nonlinear effect in the case of isoprene, emissions were reduced by 20%, and the difference between that simulation and the standard simulation was multiplied by 5.
[f] PAN production from isoprene involves additional precursors other than acetaldehyde and methylglyoxal including methyl vinyl ketone, methacrolein and other short lived oxidation intermediates.
[g] 34 Tg C as α-pinene, 16 Tg C as β-pinene, 7.3 Tg C as sabinene, and 6.1 Tg C as δ-3-carene; lifetime is calculated as a lumped species
[h] calculated using difference between global simulations with and without terpene chemistry
[i] >C_3 alkanes are emitted as a mixed butane-pentane lumped species on a carbon-weighted basis (Lurmann et al., 1986)
[j] Includes primary terrestrial and ocean sources
[k] From Fu et al. (2008)
[l] >C_2 alkenes are emitted as propene on a carbon-weighted basis

Emily Fischer 1/9/14 11:14 PM
Formatted: Superscript

[m] Photolysis of methylglyoxal produces acetaldehyde in GEOS-Chem. Calculation assumes each of two absorption bands is responsible for half of the photolysis.
[n] > Lumped species including, o-xylene, m-xylene, p-xylene, 1,2,3-trimethylbenzene, 1,2,4-trimethylbenzene and1,2,5-trimethylbenzene with the reactivity of m-xylene
[o] Also including ethylbenzene with the reactivity of toluene
[p] Chemical yield from photolysis and reaction with OH of hydroxyacetone is unity, but 18 % of hydroxyacetone is removed by wet deposition.

1322 **Table 2:** Global PAN measurements used for model evaluation listed in order of map
1323 regions labeled on Figure 2.

1324

Aircraft Missions				
Experiment	***Timeframe***	***Location***	***Figure 1 Map Regions***	***Reference***
TRACE-P	Mar-Apr 2001	W Pacific	1,2,5,6	(Talbot et al., 2003)
PEM-West B	Feb – Mar 1994	W Pacific	3	(Singh et al., 1998)
PEM-West A	Sep – Oct 1991	W Pacific	4,7,8	(Singh et al., 1996b)
PEM-Tropics B	Mar – Apr 1999	Tropical Pacific	9 - 13	(Maloney et al., 2001)
PEM-Tropics A	Aug – Oct 1996	S Pacific	14 - 17	(Talbot et al., 2000)
INTEX-B	Mar – May 2006	E Pacific	18 - 20	(Singh et al., 2009)
PHOBEA	Mar – Apr 1999	E Pacific	21	(Kotchenruther et al., 2001)
ITCT-2K2	Apr – May 2002	E Pacific	22	(Roberts et al., 2004)
MILAGRO	Mar – May 2006	Mexico	23	(Singh et al., 2009)
CITE-2	Aug - Sep 1986	W U.S.	24 - 25	(Singh et al., 1990a)
INTEX-A	Jul – Aug 2004	Eastern N America	26 - 28	(Singh et al., 2006)
SONEX	Oct – Nov 1997	N Atlantic	29, 42	(Talbot et al., 1999)
ABLE-2B	Apr - May 1987	Amazon	30	(Singh et al., 1990b)
TRACE-A	Sep – Oct 1992	S Atlantic	31-32, 43-45	(Singh et al., 1996a)
ABLE-3A	Jul –Aug 1988	Alaska	33	(Singh et al., 1992)
ABLE-3B	July – Aug 1990	E Canada	34 - 35	(Singh et al., 1994)
ARCTAS	Apr – Jul 2008	N American Arctic	36 - 38	(Alvarado et al., 2010)
ARCPAC	Mar – Apr 2008	Alaska	39	(Slusher et al., 2004)
POLARCAT	July 2008	Greenland	40	(Roiger et al., 2011)
TOPSE	Feb – Mar 2000	N American Arctic	41	(Atlas et al., 2003)
AMMA	Aug 2006	West Africa	46	(Stewart et al., 2008)
Surface Measurements				
Site Name	***Timeframe***	***Location***	***Elevation***	***Reference***
Mount Bachelor	Mar – May 2008 - 2010	44°N, 122°W	2.7 km	(Fischer et al., 2010)
Jungfraujoch	1997 – 1998, 2005 - 2006, 2008	47°N, 9°E	3.6 km	(Balzani Loov et al., 2008; Whalley et al., 2004; Zellweger et al., 2000; Pandey Deolal et al., 2013)
Hohenpeissenberg	2003 - 2008	48°N, 1°E	985 m	http://ds.data.jma.go.jp/gmd/wdcgg/
Schauinsland	1995 - 2010	48°N, 8°E	1.2 km	http://ds.data.jma.go.jp/gmd/wdcgg/
Zugspitze	2004 - 2008	47°N, 11°E	2.7 km	http://ds.data.jma.go.jp/gmd/wdcgg/
Waliguan	Jul – Aug 2006	36°N, 101°E	3.8 km	(Xue et al., 2011)
Bush Estate	1994 - 1998	56°N, 3°W	200 m	(*McFayden et al*., 2005)
Rishiri	1999	45°N, 141°E	35 m	(Tanimoto et al., 2002)
Poker Flat	Mar – May 1993, 1995	65°N, 148°W	470 m	(Beine et al., 1996)
Alert	Jan – Apr 1992, 1998, 2000	82°N, 62°W	200 m	(Dassau et al., 2004; Worthy et al., 1994)
Zeppelin	1994 - 1998	78°N, 16°W	474 m	(Beine et al., 1997; Beine and Krognes, 2000)
Polarstern Cruise	May – Jun 1998	52°N – 17°S, 7°E – 19°W	Sea level	(Jacobi et al., 1999)
Thompson Farm	2005 - 2007	43°N, 71°W	25 m	Robert Talbot, Ryan Chartier, unpublished data
Summit Greenland	Jun-Jul 1998, Jan 1999	47°N, 9°E	3.2 km	(Ford et al., 2002)
Pico Mountain	Jul – Sep 2008, Mar – Jul 2009	38°N, 28°W	2.2 km	Katja Dzepina, Jim Roberts, unpublished data

Figure Captions

Figure 1: Locations of PAN observations used in our analysis (Table 2): surface sites (red *); aircraft missions (black boxes) with region numbers indicated; and one cruise (red line).

Figure 2: Global mean distribution of PAN for different seasons and altitude ranges. Model results for 2008 (background solid contours) are compared to observations from Table 2 for all years (filled circles). Aircraft observations are averaged vertically and horizontally over the coherent regions of Figure 2.

Figure 3: Longitudinal cross-section of seasonal mean PAN concentrations at northern mid-latitudes (30 – 60 °N) as a function of altitude. Model results for 2008 (background solid contours) are compared to observations from many years in Table 2 (filled circles). Circles are placed at the mean longitude of the coherent regions (Figure 2) that fall between (30 – 60 °N).

Figure 4: Relative sensitivity of total column PAN concentrations to emissions of NO_x and NMVOCs in April and July. The sensitivity is diagnosed as $\Delta PAN/\Delta E$, where ΔPAN is the change in monthly mean PAN column concentrations resulting from a 20% decrease ΔE in global emissions of either NMVOCs (top) or NO_x (bottom), including all sources and sustained year-round. Zero indicates no sensitivity, while one indicates 1:1 sensitivity.

Figure 5: Global contributions of individual NMVOCs to PAN formation, expressed as the relative contributions to the major carbonyl species producing the peroxyacetyl radical (PA), and from there, the relative contributions of the carbonyl species to global PA production. Values are from Table 1. The geographical and vertical distribution of total PA radical production is given in Figure 6.

Figure 6: Annual total PA radical production for three altitude ranges contributed by the immediate precursors methylglyoxal, acetone, and acetaldehyde. The other precursors include a number of species produced in the oxidation of isoprene.

Figure 7: Sensitivity of PAN to different emission types. Results are shown as relative decreases of monthly mean total PAN columns in sensitivity simulations with individual emission types shut off. Biogenic signifies NMVOCs only.

Figures

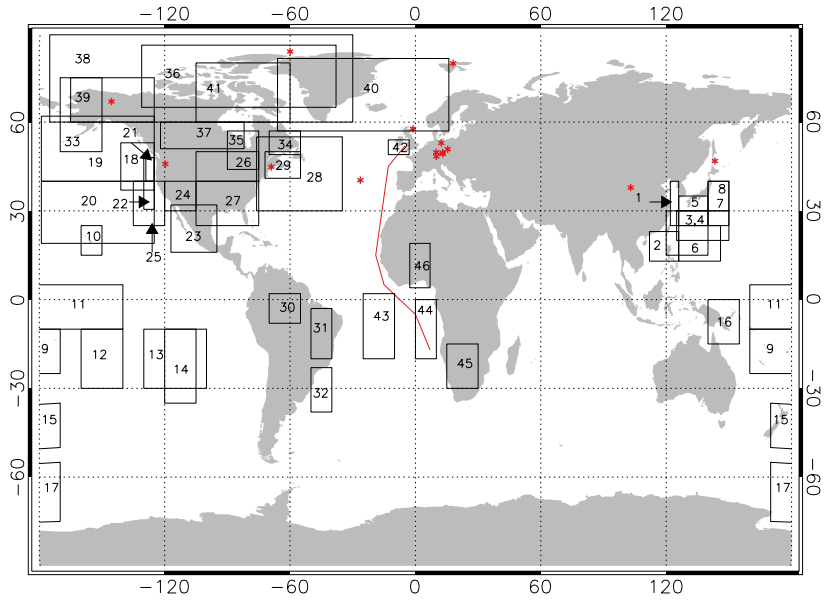

Figure 1: Locations of PAN observations used in our analysis (Table 2): surface sites (red *); aircraft missions (black boxes) with region numbers indicated; and one cruise (red line).

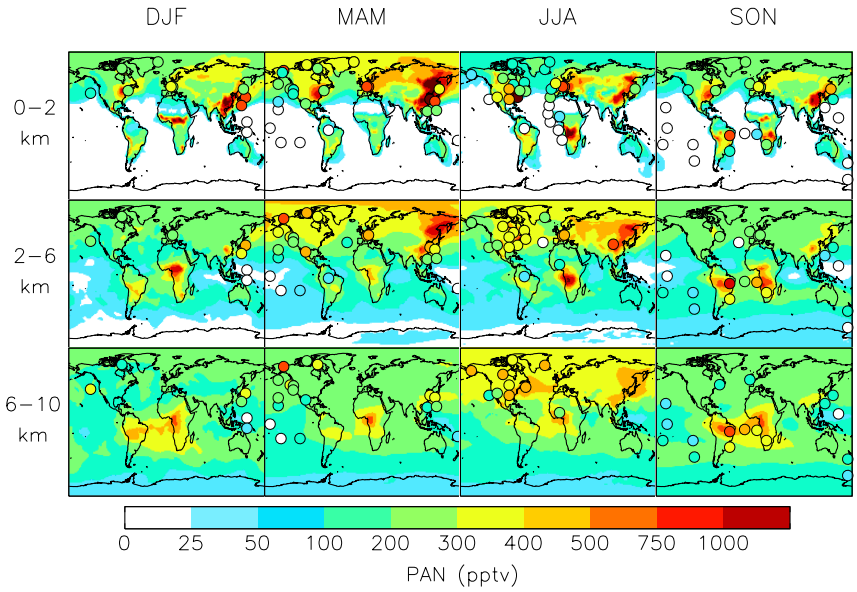

Figure 2: Global mean distribution of PAN for different seasons and altitude ranges. Model results for 2008 (background solid contours) are compared to observations from Table 2 for all years (filled circles). Aircraft observations are averaged vertically and horizontally over the coherent regions of Figure 2.

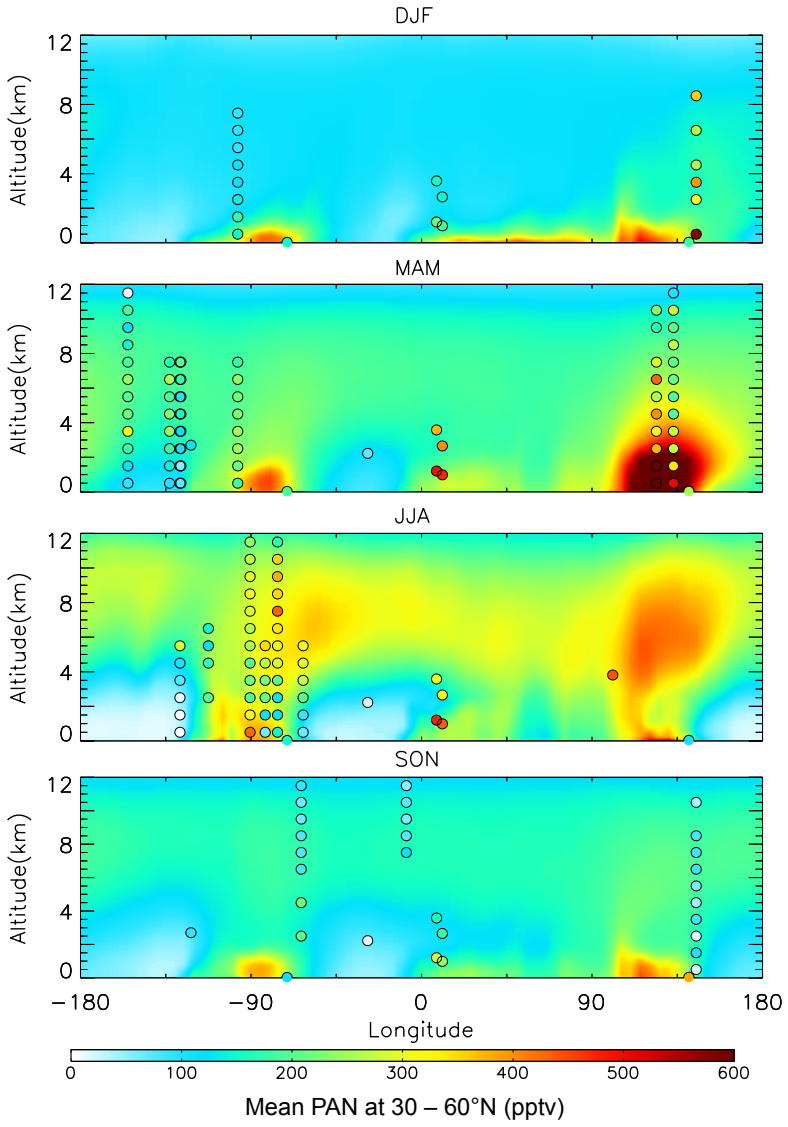

Figure 3: Longitudinal cross-section of seasonal mean PAN concentrations at northern mid-latitudes (30 – 60 °N) as a function of altitude. Model results for 2008 (background solid contours) are compared to observations from many years in Table 2 (filled circles). Circles are placed at the mean longitude of the coherent regions (Figure 2) that fall between (30 – 60 °N).

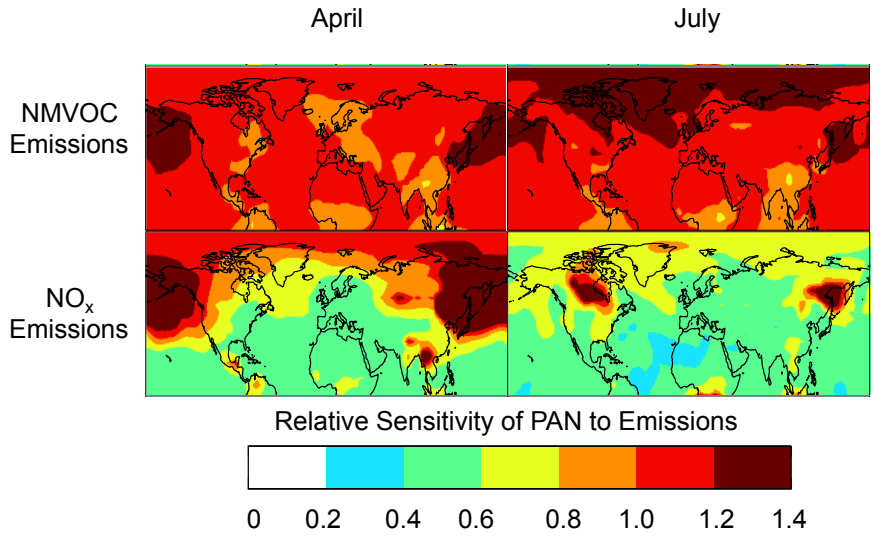

Figure 4: Relative sensitivity of total column PAN concentrations to emissions of NO_x and NMVOCs in April and July. The sensitivity is diagnosed as $\Delta PAN/\Delta E$, where ΔPAN is the change in monthly mean PAN column concentrations resulting from a 20% decrease ΔE in global emissions of either NMVOCs (top) or NO_x (bottom), including all sources and sustained year-round. Zero indicates no sensitivity, while one indicates 1:1 sensitivity.

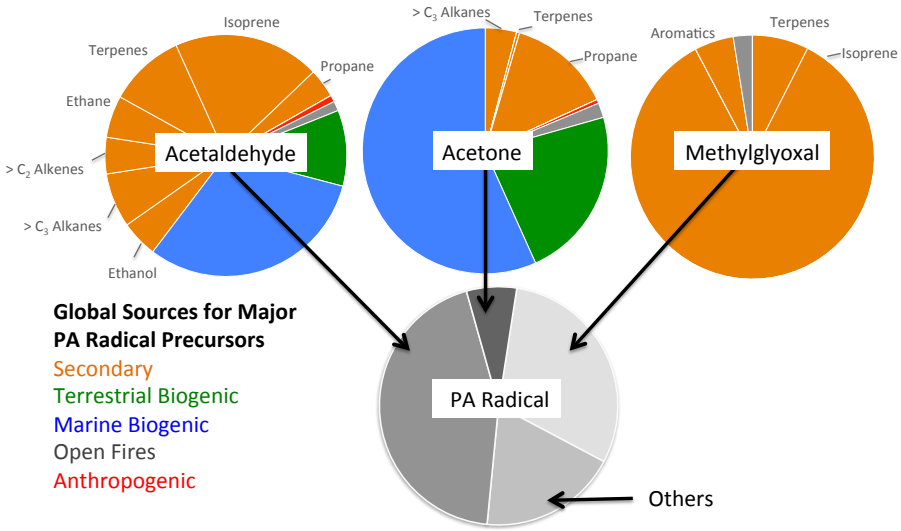

Figure 5: Global contributions of individual NMVOCs to PAN formation, expressed as the relative contributions to the major carbonyl species producing the peroxyacetyl radical (PA), and from there, the relative contributions of the carbonyl species to global PA production. Values are from Table 1. The geographical and vertical distribution of total PA radical production is given in Figure 6.

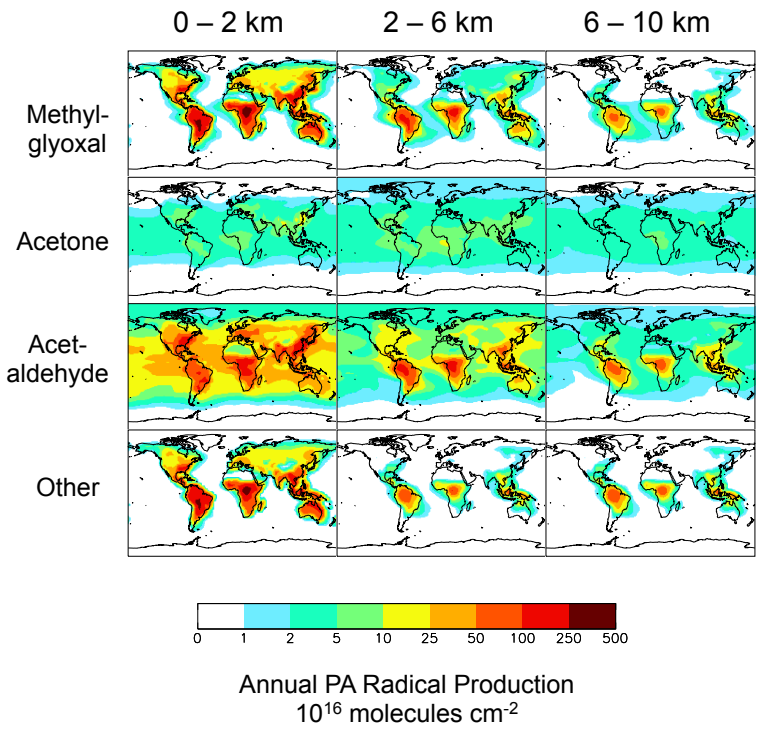

Figure 6: Annual total PA radical production for three altitude ranges contributed by the immediate precursors methylglyoxal, acetone, and acetaldehyde. The other precursors include a number of species produced in the oxidation of isoprene.

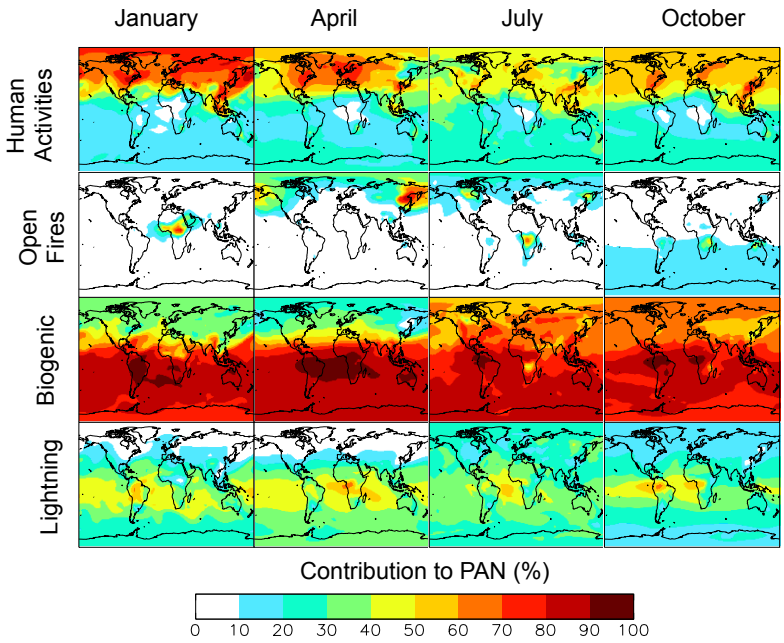

Figure 7: Sensitivity of PAN to different emission types. Results are shown as relative decreases of monthly mean total PAN columns in sensitivity simulations with individual emission types shut off. Biogenic signifies NMVOCs only.

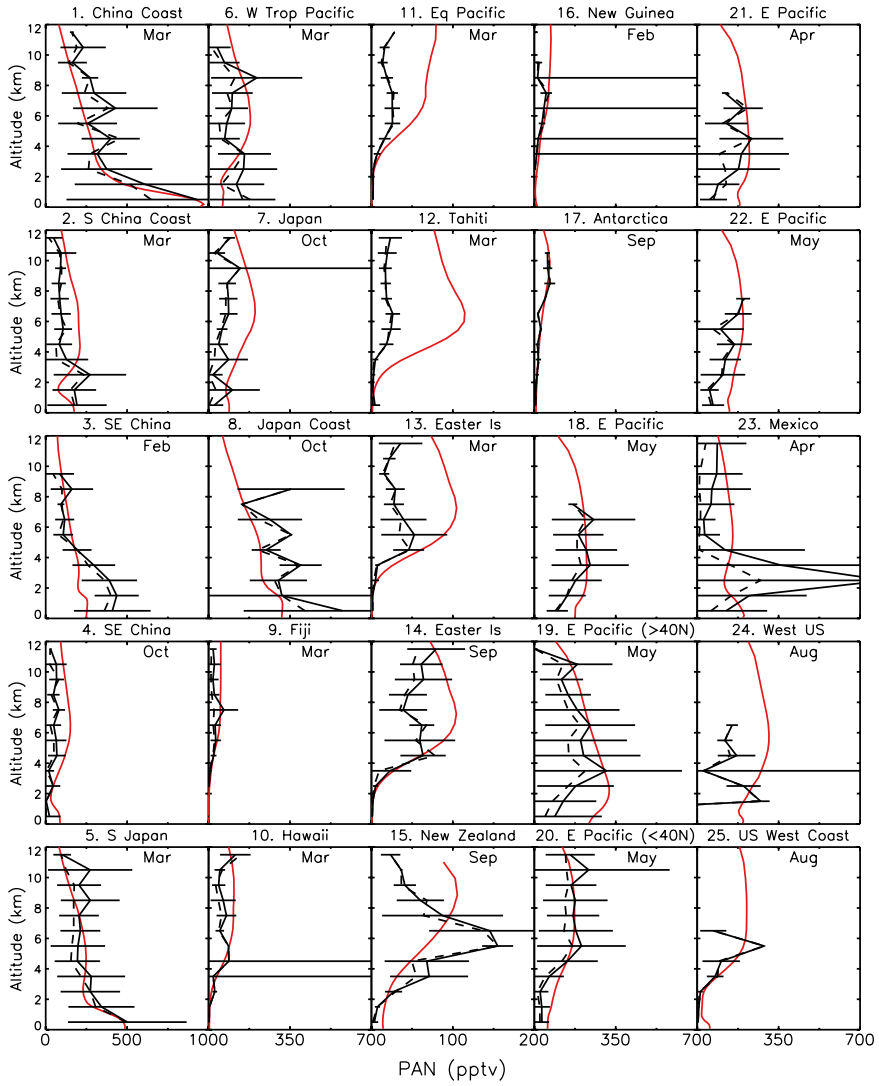
1. China Coast
Mar
6. W Trop Pacific
Mar
11. Eq Pacific
Mar
16. New Guinea
Feb
21. E Pacific
Apr
2. S China Coast
Mar
7. Japan
Oct
12. Tahiti
Mar
17. Antarctica
Sep
22. E Pacific
May
3. SE China
Feb
8. Japan Coast
Oct
13. Easter Is
Mar
18. E Pacific
May
23. Mexico
Apr
4. SE China
Oct
9. Fiji
Mar
14. Easter Is
Sep
19. E Pacific (>40N)
May
24. West US
Aug
5. S Japan
Mar
10. Hawaii
Mar
15. New Zealand
Sep
20. E Pacific (<40N)
May
25. US West Coast
Aug
Altitude (km)
0 2 4 6 8 10 12
0 500 1000 350 700 100 200 350 700 350 700
PAN (pptv)

1430

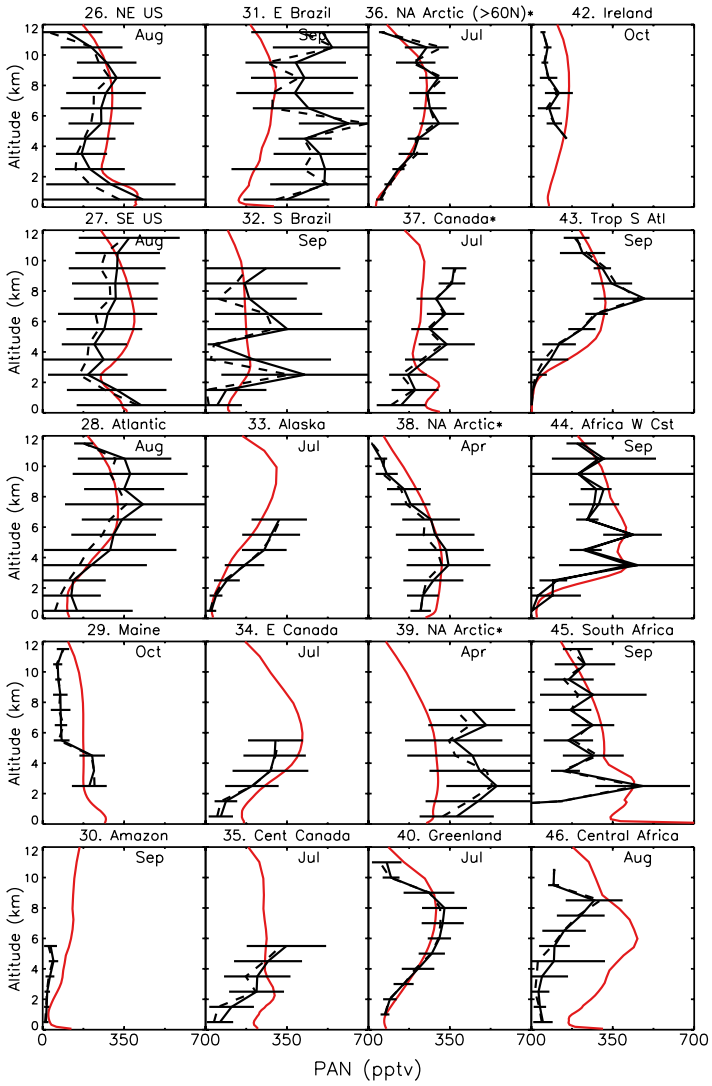

Figure S1: Vertical profiles of PAN for the regions in Figure 1 and Table 1. Symbols and horizontal bars are mean and standard deviations of aircraft observations. The model results (red lines) calculated using GEOS-5 for 2008, are monthly mean values for the flight regions. * Indicates that the data has been filtered to remove biomass burning plumes.

Different filters were applied for each dataset following the analysis of Liang et al. (2011) and Brock et al. (2011). Biomass burning plumes were identified in ARCTAS-A as samples with CH_3CN > 145 pptv and CO > 160 ppbv, in ARCTAS-B as samples with CH_3CN > 320 pptv and CO > 120 ppbv, and in ARCPAC as samples with CH_3CN > 100 pptv and CO > 170 ppbv. Only marine data and model results west of 125°W have been included for INTEX-B and ITCT-2K2. Transit flights, where the San Francisco and Los Angeles plumes were encountered, were also removed from the ITCT-2K2 data. Note the differences in scales between panels.

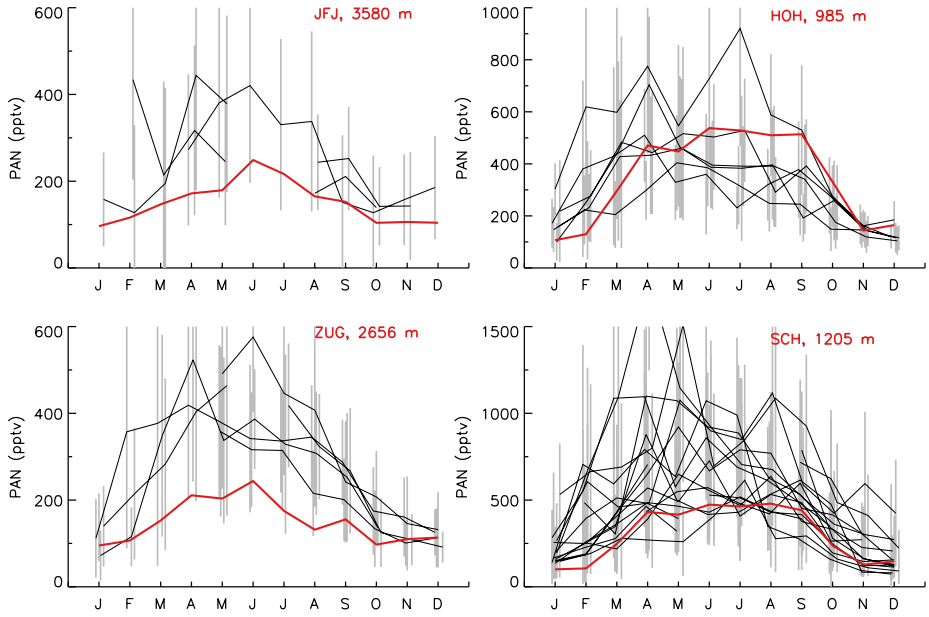

Figure S2: PAN mixing ratios for European mountaintop sites: Jungfraujoch (JFJ), Zugspitze (ZUG), Hohenpeissenberg (HOH) and Schauinsland (SCH). Black lines are monthly mean observed values over many years (Table 1). Grey vertical bars are standard deviations for each monthly mean. The model results (red lines) are monthly mean values for 2008.